Quaternary Science Reviews 120 (2015) 28–46

Contents lists available at ScienceDirect

Quaternary Science Reviews

journal homepage: www.elsevier.com/locate/quascirev

Invited review

Interglacial analogues of the Holocene and its natural near future

Qiuzhen Yin*, André Berger

Georges Lemaître Center for Earth and Climate Research, Earth and Life Institute, Université catholique de Louvain, Louvain-la-Neuve, Belgium

ARTICLE INFO

Article history:
Received 29 July 2014
Received in revised form
7 April 2015
Accepted 8 April 2015
Available online

Keywords:
Interglacials
Climate analogue
Insolation
CO_2
Paleoclimate modelling
Astronomical theory of paleoclimates

ABSTRACT

In an attempt to find potential interglacial analogues of our present interglacial and its natural future, five interglacials (MIS-1, 5, 9, 11 and 19) are studied in terms of their astronomical characteristics, greenhouse gases concentration and climate simulated using both snapshot and transient experiments. Transient simulations covering a full range of obliquity, precession and eccentricity allow to develop an OPE index to estimate the climate sensitivity to astronomical forcing. They also show that obliquity and precession have different weight on the annual mean temperature and precipitation of different latitudinal zones, leading to varying phasing of these climate variables between different latitudes. However, the variations in boreal summer temperature of different latitudes (except the Southern Ocean) are in phase and are dominated by precession. All the interglacials are shown to be warmer than the natural climate of the present day and of the next centuries during boreal summer and for the annual mean temperature with varying duration and intensity. Such warming is mainly caused by changes in insolation, unlike the present global warming which mainly results from anthropogenic CO_2 increase. The exceptionally long duration of MIS-11 is confirmed by our simulations, and it is demonstrated to be related to the long-lasting low eccentricity and high CO_2 concentration and to the anti-phase relationship between obliquity maximum and precession minimum during MIS-11. As far as the variations of annual and seasonal temperatures are concerned, both snapshot and transient simulations show that MIS-19 is the best analogue of the present interglacial. MIS-11 is also a decent analogue when the impact of insolation alone is considered, but it is warmer than MIS-1 when the impact of CO_2 is additionally included. Due to the large amplitude in the variations of insolation, MIS-5 and MIS-9 can hardly be considered as an analogue of the natural present-day climate and of its near future, but such warm climates could be, at least partly, considered as analogues of the future man-made warm climate. Although their astronomical forcing is different from the future and their CO_2 concentration is much lower, the past interglacials have similarities to the anthropogenic warming in terms of climate feedbacks at the regional scale.

1. Introduction

As we are presently in an interglacial, the Holocene, that is moreover predicted to be exceptionally long (Berger and Loutre, 1996, 2002), past interglacials are particularly relevant to better understand our present-day warm climate and hopefully its future. They provide a quite complete view of the range and underlying physics of natural warm climate variability. They also provide insights into climate processes and feedbacks during warm intervals. In addition, the climate predicted to occur over the next centuries (IPCC, 2013) appears to be unprecedented over the last 150 years. Past climate offer therefore the other unique opportunity to test, over a wide range of situations, the reliability of the climate models used for projecting the climate of the next centuries. It is expected that this will help to improve our estimate of the sensitivity of the climate system. As the past interglacials are the most recent warm periods in the Earth's history, they have often been studied in order to know if they might provide analogues of the future climate with a reasonable estimate of the seasonal and geographical description of what might happen in the centuries to come. Interglacial analogues might also give indications about the length of our current interglacial and therefore when it will end.

The interglacial MIS-11 about 400 ka ago (Berger and Loutre, 2002, 2003) and the Last Interglacial about 125 ka ago (corresponding to MIS-5e, MIS-5 in short here) (Kukla et al., 1997) have long been considered as the analogues of the Holocene and its

* Corresponding author.
E-mail address: qiuzhen.yin@uclouvain.be (Q.Z. Yin).

http://dx.doi.org/10.1016/j.quascirev.2015.04.008
0277-3791/

future. MIS-5 was indeed characterized by higher temperature in many parts of the Northern Hemisphere (NH) (eg. CAPE, 2006), higher global sea level (eg. Kopp et al., 2009) and reduced ice sheets (eg. Otto-Bliesner et al., 2006; NEEM, 2013), all features which are consistent with the IPCC predictions of the response of the climate system to human impacts. However, MIS-5 as a modern analogue was questioned by Berger (1989) and in Loutre and Berger (2003) because of its totally different astronomical configuration from today and the near future. MIS-11, which also had higher sea level and smaller ice sheets as indicated by proxy records (eg. Olson and Hearty, 2009; Raymo and Mitrovica, 2012), was proposed to be the best astronomical analogue of the Holocene mainly due to their similar very low values of eccentricity and consequently of their similar latitudinal and seasonal distributions of insolation (Berger and Loutre, 2002, 2003; Loutre and Berger, 2003). Climate simulations (Berger and Loutre, 2002) show that our present interglacial might naturally last very long like MIS-11. MIS-11 was confirmed to be such an appropriate analogue for the Holocene and its future by marine sediments from North Atlantic (McManus et al., 2003), but was questioned by Bauch et al. (2000) based on marine sediments from the Nordic Seas. This underlines the complexity of looking for analogues at a regional scale and leads to recommend using first global scale phenomena to look for similarities.

From the phasing between precession and obliquity and the caloric summer half-year insolation, Ruddiman (2007) suggested MIS-9 being the closest insolation analogue of the Holocene. An in-phase relationship between maximum obliquity and minimum precession (NH summer at perihelion) for MIS-9 and MIS-19 was also stressed by Yin and Berger (2010) leading to a large summer insolation in the NH, although reduced by a moderate eccentricity value. In parallel, Yin and Berger (2012) have shown that MIS-9 is the simulated warmest interglacial among the last nine ones as a result of both its high CO_2 concentration and its insolation configuration. Finally, attention has been paid to the interglacial MIS-19 about 780 ka ago (Berger and Loutre, 1996; Pol et al., 2010; Tzedakis, 2010, 2012; Yin and Berger, 2010, 2012), a time when eccentricity was minimum, like for MIS-11, for MIS-1 and mainly its future, related to the dominant 400-ka cycle in eccentricity (Berger, 1978). Considering MIS-19 as a good analogue of the Holocene, Tzedakis et al. (2012) suggested that the current interglacial would end within the next 1500 years if the CO_2 concentration would not exceed 240 ppmv.

Looking for analogues involves the intercomparison of the interglacials not only at the global scale but also at the regional one. For example, Masson-Delmotte et al. (2010) compared the intensity of the interglacials from Antarctica and found that MIS-5 and MIS-11 were the warmest followed by MIS-9 and MIS-1. The data compilation of Lang and Wolff (2011) shows that the interglacial intensity varies in space and depends on variables, with MIS-5 being generally the strongest. Tzedakis et al. (2009) using several proxy records also found that palaeoclimates of the past 800 ka reveal a large diversity among interglacials in terms of their intensity, duration and internal variability. Past interglacials were also intercompared using climate simulations. Snapshot experiments have been made to simulate the climate of the last nine interglacials (from MIS-1 to MIS-19) with an Earth system model of intermediate complexity (LOVECLIM) (Yin and Berger, 2010, 2012; Yin, 2013). Yin and Berger (2010) and Yin (2013) focused on the differences between the pre-MBE and the post-MBE interglacials, whereas Yin and Berger (2012) analysed the pure contributions of insolation and Greenhouse Gases (GHG, here including CO_2, CH_4 and N_2O), as well as their combined effects to the climate of the last nine interglacials. Using the same forcing, Herold et al. (2012) simulated the climate of the five warmest interglacials with the NCAR atmosphere-ocean general circulation model (CCSM3).

Although the analogue of present and future climate has long been looked for from the past interglacials, caution should be taken because the highest CO_2 concentration of the interglacials of the past 800 ka is not more than 300 ppmv, which is much lower than the anthropogenic CO_2 concentration of more than 500 ppmv projected to occur in the next centuries (IPCC, 2013). In addition, Yin and Berger (2012) showed that the northern hemisphere warming during the past interglacials originates mainly from high boreal summer insolation. Ganopolski and Robinson (2011) also showed that, different from the present-day global warming which is caused by high concentration of greenhouse gases, the warmth of MIS-5 results mainly from high summer insolation in the northern hemisphere, questioning the suitability of MIS-5 as an analogue for the future climate. According to Van de Berg et al. (2011), a large part of the Greenland ice sheet melting during the Last Interglacial is not related to higher ambient temperature but caused by higher summer insolation and associated nonlinear feedbacks. They suggested that projections of future Greenland ice loss on the basis of Eemian temperature–melt relations may overestimate the future vulnerability of this ice sheet.

It is therefore obvious that the past interglacials cannot be considered as straightforward analogues of the present and the future climate which is primarily controlled by anthropogenic high CO_2 concentration. However, given the similarity in astronomical configurations between some past interglacials and the present and the future, it is reasonable to look for past interglacial analogues for the natural climate of Holocene and its future. In this paper, we compare the past interglacials to the natural climate of the Holocene and its near future using climate simulations and try to identify the interglacial(s) which is (are) the closest to the “natural” present and future in terms of both climatic optima and variations. This is expected to help better assess the impacts of human activities against the natural climate background.

In the snapshot simulations of previous studies (Yin and Berger, 2010, 2012; Herold et al., 2012; Yin, 2013), the forcings selected at specific dates were assumed to simulate the “Optimum” of each interglacial but only under certain hypothesis. In this study, another set of snapshot simulations with insolation different from that used in these previous studies is performed to assess which date is the best for selecting the insolation to simulate the interglacial Optima when snapshot experiments are used. In search of analogues of the Holocene, it is important to compare the interglacials not only for their “Optima” but also over their entire periods. Transient simulations are therefore also performed to obtain the climate response to a full spectrum of astronomical configurations during the entire period of each interglacial (see Section 2 for details). These additional snapshot and transient simulations together with some snapshot simulations from Yin and Berger (2012) are used here to compare MIS-5, MIS-9, MIS-11 and MIS-19 to MIS-1 and its natural near future looking for analogues in terms of interglacial forcing and the simulated climate responses. The strategy used for modelling the interglacials is introduced in Section 2. The characteristics of the astronomical parameters and insolation of the five interglacials are shown in Section 3. The snapshot simulations in which the insolation of NH summer occurring at perihelion (NHSP) is used are discussed in Section 4. In Section 5, the snapshot simulations in which the insolation at the interglacial $\delta^{18}O$ peaks is used are analysed and compared to the NHSP simulations of Section 4. The results of the transient climate response to astronomical forcing are given in Section 6. In Section 7, the results of the transient simulations forced by both GHG and insolation are compared to the natural climate of the present-day and the near future. Finally, conclusions are given in Section 8.

2. Model and strategies

The simulations used in this study are performed with LOVECLIM, a three dimension Earth system model of intermediate complexity (Goosse et al., 2010). It includes five components of the climate system, but here only the atmosphere (ECBilt), the ocean-sea ice (CLIO) and the terrestrial biosphere (VECODE) are interactively coupled. ECBilt is a quasi-geostrophic atmospheric model with 3 vertical levels and a T21 horizontal resolution. CLIO is made up of an ocean general circulation model coupled to a comprehensive thermodynamic-dynamic sea-ice model. Its horizontal resolution is 3° by 3°, and there are 20 vertical levels in the ocean. VECODE is a reduced form model of vegetation dynamics and of the terrestrial carbon cycle. LOVECLIM has been used in many climate studies for the past, present and future. Like every model, it has its own advantages and biases. Due to its intermediate complexity, LOVECLIM is especially suitable for performing long transient simulations and large ensemble of simulations, as required by this study. The most serious biases include an overestimation of temperature at low latitudes, an overestimation of precipitation and vegetation cover in the subtropics, and a weak atmospheric circulation (Goosse et al., 2010). In addition, compared to many models, LOVECLIM has a low climate sensitivity (1.9 °C) and a higher polar amplification, the combination of which actually leads to polar temperature changes for a given radiative forcing in line with more comprehensive AOGCMs (Goelzer et al., 2010).

The forcings considered here are the GHG concentrations and the latitudinal and seasonal distribution of insolation. Snapshot experiments are often used in paleoclimate modelling. The difficulty of making a snapshot experiment is to select the most appropriate forcing which will best reproduce a given climate, because a snapshot experiment provides the climate which is in equilibrium with the forcing used. As the real climate is never in equilibrium, the selection of the forcing deserves therefore a serious attention. As we are interested in simulating the interglacial climate “Optimum” (or hypsithermal), the maximum GHG values have been used (Table 1) for each interglacial to maximize the climate response. Due to large uncertainty in the ice sheet reconstruction during past interglacials, their present-day configuration is prescribed in all experiments. This is in agreement with their small change at the interglacial “Optima”, change which appears having little impact on the simulated global mean climate during the Last Interglacial at least (Loutre et al., 2014). Such a working hypothesis might be acceptable for the snapshot simulations which aim to simulate the interglacial “Optima” and for the periods around the interglacial peaks in the transient simulations, but it is certainly not reflecting reality for the times of deglaciation and glacial inception covered by the transient simulations. For example, the changes in ice sheets and related freshwater fluxes could have a significant impact on the global and regional temperature response (eg. Renssen et al., 2009). As a consequence, we do not intend to discuss the impact of any possible ice sheet during the times of glacial inception or deglaciation. Our transient simulations have therefore to be considered as sensitivity experiments for understanding the impact of insolation and GHG.

For insolation, due to its strong seasonal and regional character, it is less evident to decide at which date to choose insolation. For example, the insolation at both 6 ka BP and 9 ka BP has been used to simulate the Holocene climate (eg. Kutzbach, 1981; Hewitt and Mitchell, 1998), and several different dates have been used for the Last Interglacial simulations (eg. Lunt et al., 2013). Due to such difficulty, we use here three strategies to simulate the climate of MIS-1, -5, -9, -11 and -19:

- Snapshot experiments with insolation at a date when boreal summer occurred at perihelion
- Snapshot experiments with insolation at the interglacial $\delta^{18}O$ peaks
- Transient experiments with time-varying insolation: one set with GHG concentration fixed at their Pre-Industrial (PI) level, and another with time-varying GHG

For the snapshot experiments in the first and second strategies, the model integration is 1000-yr long. This leads to an equilibrium climate state at the end of the simulations and the last 100-year climatology is analysed.

The first strategy was explained in detail in Yin and Berger (2012). It is briefly summarized here. First, the peaks of the interglacials were selected from the marine $\delta^{18}O$ records (Table 1) which are supposed to be of global significance and are the basis for defining glacial–interglacial stages. However, it must be stressed that such peaks do not necessarily represent the warmest climate, the $\delta^{18}O$ records being primarily a function of the global ice volume, but also of deep-ocean temperature. Second, following the hypothesis that an interglacial is associated with a maximum insolation in the NH during its summer (Kukla et al., 1981), the astronomical parameters (Berger, 1978) were taken at the dates when NH summer occurs at perihelion just preceding the $\delta^{18}O$ peaks. This choice of insolation could be further justified by a constant phase relationship between precession minima (NHSP) and the interglacial peaks in the proxies of global significance like in the marine $\delta^{18}O$ records (eg. Lisiecki and Raymo, 2005), in the simulated NH minimum ice volume (Ganopolski and Calov, 2011) and in the compiled maximum global sea level (Kopp et al., 2009). The climate proxies lag behind precession by about 5 ka, which reflects the response time of the slow processes in the climate system to the astronomically induced insolation. This lag means also that the $\delta^{18}O$ peaks occur close to a time when fall equinox occurs at perihelion. Moreover, another reason of selecting the date of NHSP is to maximize the NH summer insolation. It must be stressed that, by no means, we intend to simulate the climate at the date of NHSP. It is definitely the climate Optimum of each interglacial that is attempted to be reproduced by selecting the insolation of NHSP. The pure contributions of insolation and GHG have

Table 1
Dates, astronomical parameters and CO_2 equivalent concentration of the two sets of snapshot simulations as well as the time periods covered by the two sets of transient simulations. Astronomical parameters are from Berger (1978) and the dates of the benthic $\delta^{18}O$ peaks are from Lisiecki and Raymo (2005).

Marine isotope stage	Snapshot simulations							Time period covered by transient simulations (ka BP)
	Date of NH summer at perihelion (ka BP)	Eccentricity	Obliquity	Date of $\delta^{18}O$ peaks (ka BP)	Eccentricity	Obliquity	CO_{2eq} (ppmv)	
MIS-1	12	0.019608	24.15	6	0.018682	24.11	264	17 ka BP – 3 ka AP
MIS-5	127	0.039378	24.04	123	0.040531	23.50	284	133–111
MIS-9	334	0.031539	24.24	329	0.035021	24.01	300	340–318
MIS-11	409	0.019322	23.78	405	0.019535	23.21	286	425–394
MIS-19	788	0.026196	24.00	780	0.024336	23.55	265	793–773

been estimated by using the factor separation method (Yin and Berger, 2012).

In the attempt to simulate the interglacial climate Optimum, the insolation at the date of the interglacial peak has sometimes also been used. For example, the insolation at 6 ka BP has been used to simulate the Holocene Optimum in the Paleoclimate Modelling Intercomparison Project (PMIP) (eg. Joussaume and Taylor, 1995; Braconnot et al., 2007) due to availability of proxy data and similarity in ice sheets between that time and today. Our second strategy was therefore to model the climate response to the insolation forcing taken at the dates of the interglacial $\delta^{18}O$ peaks (Table 1). The same GHG concentrations as in the first strategy are used for an easier comparison and to maximize the forcing, the idea being again to attempt reproducing the climate Optimum.

The snapshot simulations at the interglacial $\delta^{18}O$ peak and at the time of NHSP represent only two single time slices within the whole interval of each interglacial. The insolation at these dates is assumed to simulate the "Optimum" of each interglacial but only under certain hypotheses (Yin and Berger, 2010). To obtain the climate response to a full spectrum of astronomical configurations during the entire period of each interglacial and to set the snapshot simulations back in a broader context, the third strategy was to make transient simulations for the five interglacials. In a first set of experiments, only insolation is allowed to vary with time, the GHG concentrations being fixed to their PI level ($CO_2 = 280$ ppmv). This allows to estimate the sensitivity of the interglacials to the astronomical forcing only and ensures a first easier intercomparison. In the second set of experiments, both the insolation and GHG vary continuously with time. The simulations for MIS-1, -5, -9, and -19 cover one precession cycle and start at the dates when NH spring occurs at perihelion just before the $\delta^{18}O$ peak of the interglacials (Table 1). The simulation of MIS-1 covers the future 3 ka but only in the first set of experiments. As MIS-11 has a longer duration (Berger and Loutre, 2003; Jouzel et al., 2007), its simulation covers 10 ka more, starting at 425 ka BP when NH fall occurs at perihelion, i.e. one precessional cycle earlier than the $\delta^{18}O$ peak at 405 ka BP. The initial conditions of these transient simulations are equilibrium states calculated from 2000-year long integrations performed at the starting dates (Table 1) of the transient simulations.

Although being a model of intermediate complexity, LOVECLIM remains still costly for transient experiments, particularly when 5 interglacials and 10 transient simulations are considered. An acceleration technique similar to Lorenz and Lohmann (2004) was therefore used to speed up the simulations and reduce the computational costs. An acceleration factor of 10 is used, which means that at the end of each year of the simulation, the astronomical parameters and GHG concentration are advanced by 10 years. In such a case, the actual length of the simulation is reduced by 10 times. For example, a 20,000-year long simulation only needs 2000 model years. To test the impact of such an acceleration technique on our transient simulations, a non-accelerated experiment and a 10-time accelerated one have been done for two interglacials MIS-5 and MIS-13. Our results showed that the acceleration method has little impact on the surface air temperature and precipitation. However, the response of the deep-ocean temperature is delayed by 2–3 ka in the accelerated simulations as compared to the non-accelerated ones, similar results being observed also in other studies (Timm and Timmermann, 2007; Ganopolski and Calov, 2011). A detailed analysis made by Timm and Timmermann (2007) shows that a 10-time acceleration leads to a delayed response of the temperature only in the inner ocean. As here we are mainly interested in surface climates, the 10-time acceleration technique would not alter our conclusion about the phasing between the surface temperatures of different regions.

3. Characteristics of the astronomical parameters and insolation of the five interglacials

In the insolation forcing, both the amplitude of the astronomical parameters and the phase relationship between them play a role. When precession minimum (NHSP) and obliquity maximum are in phase, the insolation in northern high latitudes during boreal summer is strengthened and it might be expected that this would lead to strong interglacials. It is therefore interesting to analyse first this phase relationship between precession and obliquity for each interglacial. For MIS-1, MIS-9 and MIS-19, precession minimum and obliquity maximum are more or less in phase (Fig. 1a), leading the $\delta^{18}O$ minimum (named here the interglacial $\delta^{18}O$ peak) by a few thousands of years. The obliquity maximum of MIS-1 occurred 3 ka later than precession minimum, whereas at MIS-5 it occurred 4 ka earlier. For MIS-11 the precession minimum lags behind the obliquity maximum by 8 ka, making them almost in opposite phase. As a conclusion, as far as the phase relationship between precession and obliquity is concerned, MIS-9 and MIS-19 are the closest to MIS-1.

About the amplitude of the astronomical parameters, it must be stressed first that the most important contribution to the long-term variations of the daily insolation (used to force the climate models) is from precession (Berger et al., 2010). Although obliquity plays a more important role in the high latitudes than in the low ones, it never dominates the precession signal except close to the polar night where, however, the energy available is insignificant. In our first and second strategies where the longitude of the perihelion is pretty similar from one interglacial to another, it is the long-term variations of eccentricity which are of primary interest. Berger (1978) showed that the main spectral component of eccentricity is a period of about 400 ka and that the orbit of the Earth around the Sun will become circular at 27 ka AP. An analogue situation is therefore found about 400 ka ago during MIS-11 (Berger and Loutre, 1996, 2003) with eccentricity remaining pretty low. The previous analogue is about 800 ka ago during MIS-19. It must be stressed here that eccentricity remains pretty low during MIS-1, MIS-11 and MIS-19 over an interval of time at least as long as one precession cycle. Over these low-eccentricity intervals, the precession parameter ($e \sin \omega$) remains therefore small as well as its amplitude variation. Given that the eccentricity values are quite large for the other interglacials, in particular at MIS-5 and MIS-9, only MIS-11 and MIS-19 can be accepted as an eccentricity/precession analogue of MIS-1.

As far as obliquity is concerned, an unexpected result obtained by Yin and Berger (2012) was its high correlation with the insolation-induced global annual mean temperature. A large obliquity leads to a large annual irradiation at high latitudes of both hemispheres and to a lower one over the rest of the Earth (Berger et al., 2010). Although these higher and lower insolations compensate at least partly at the annual scale, the stronger response of the high latitudes due to the positive snow-ice-albedo feedback explains the net effect of obliquity on global annual temperatures. For the situation of NHSP, the obliquity of the five interglacials range between 23.78 for MIS-11 to 24.24 for MIS-9 (Table 1). Considering the time variation of obliquity, MIS-9 is the closest to MIS-1 (Fig. 1a) leading to their total irradiations over any interval of a year being similar (Berger et al., 2010), a similarity which was also pointed out by Ruddiman (2007).

The astronomical parameters are important mostly because they shape the latitudinal and seasonal distribution of insolation. This daily insolation for a single time slice is usually used in snapshot simulations. The analysis of such insolation at the dates when NH summer occurs at perihelion leads to several groups of

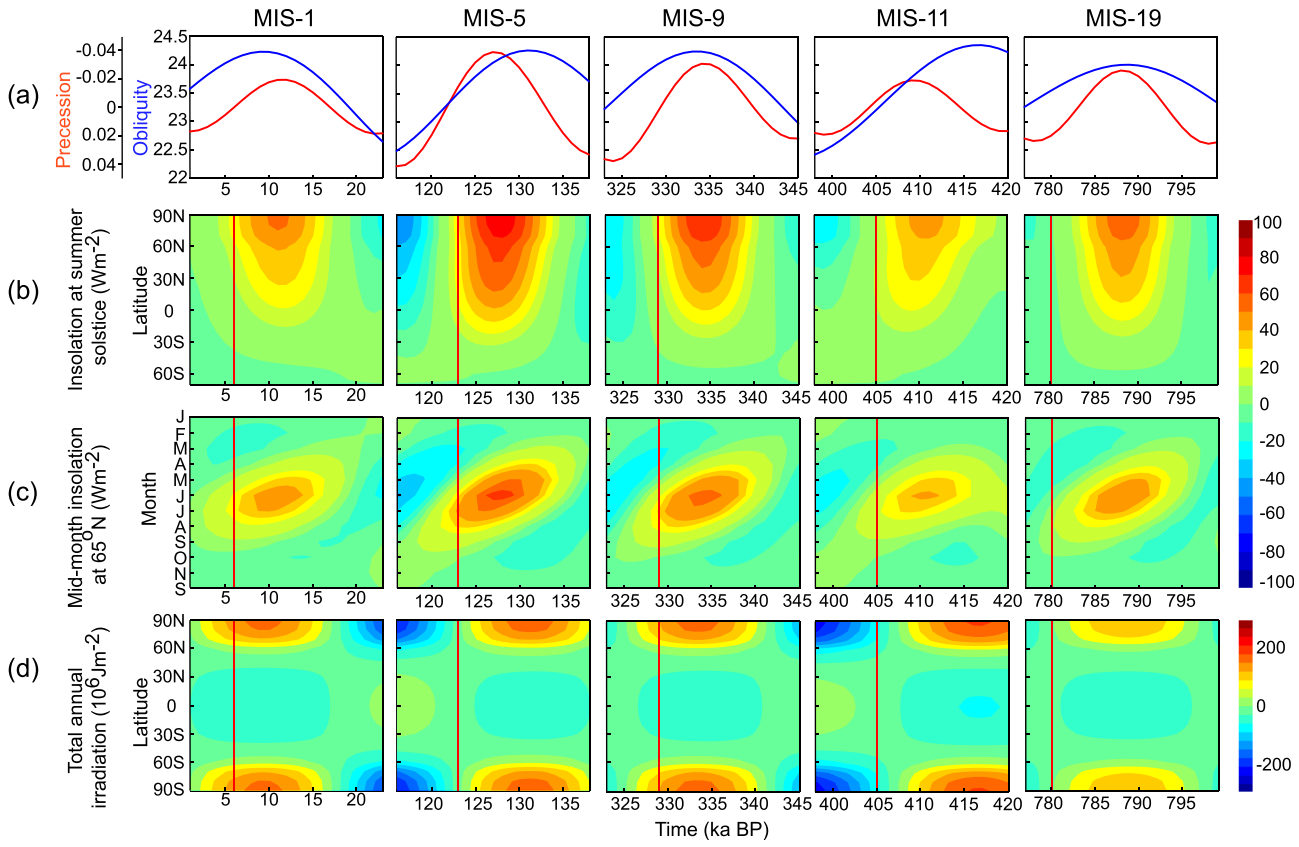

Fig. 1. Time-dependent variations of astronomical parameters and insolation of MIS-1, MIS-5, MIS-9, MIS-11 and MIS-19. (a) Precession and obliquity (°), (b) insolation (Wm^{-2}) at summer solstice for all latitudes, (c) mid-month insolation (Wm^{-2}) at 65°N, and (d) total annual irradiation (10^6 Jm^{-2}) for all latitudes. The vertical red line in (b), (c) and (d) indicates the date of the marine $\delta^{18}O$ peak of each interglacial. Insolation is calculated from the long-term variations of eccentricity, precession and obliquity (Berger, 1978).

interglacials based on their similar insolation patterns (as seen clearly from Fig. 6 of Yin and Berger, 2012). MIS-1, MIS-11 and MIS-19 were shown similar due to their low eccentricity, MIS-11 departing from MIS-1 and MIS-19 mainly because of its lower obliquity. The climate system being driven by the long-term variations of the seasonal-latitudinal distribution of insolation, it is necessary, in addition to the insolation distribution at a given date (like in Yin and Berger, 2012), to analyse also the insolation distribution as a function of time. This is illustrated in Fig. 1b–c and discussed in the following paragraphs.

First, the long term variations of daily insolation are documented in terms of the latitudinal distributions of insolation at the summer solstice (Fig. 1b) and the annual cycle of the mid-month insolation at 65°N (Fig. 1c). For these types of daily insolation, all the interglacials exhibit a similar pattern when compared to today. At the summer solstice, a positive anomaly occurs before the interglacial $\delta^{18}O$ peaks, covers the whole Earth and lasts more than 10 ka. The time evolution of the mean summer irradiance (Berger et al., 2010; figure not shown) is very similar to that of the insolation at the summer solstice except that its maximum occurs 1 or 2 ka later and is shifted towards lower latitudes. This underlines the problem raised by the choice of the insolation parameter when it is compared with proxy records or used to tune them, the timing being different from one parameter to another by a non-negligible amount. For the annual cycle of the mid-month insolation at 65°N (Fig. 1c), a maximum insolation occurs before the interglacial $\delta^{18}O$ peaks drifting from April to July over a period of more than 10 ka. The accumulation of energy during these months might be decisive for the occurrence of the interglacial $\delta^{18}O$ peaks. After the $\delta^{18}O$ peaks, the insolation maximum occurs in boreal fall and winter, and the minimum in boreal spring and summer (Fig. 1c). Such a situation would lead to mild winter and cool summer, a favourable condition for the appearance of a glaciation according to the Murphy-Milankovitch hypothesis (Berger, 2012).

As the daily insolation is mainly a function of precession (Berger, 1978), the amplitude of its variation is therefore mainly controlled by eccentricity, which means that the interglacials of higher eccentricity receive more insolation during boreal summer. For daily insolation, the amplitudes of the positive anomalies of MIS-1, MIS-11 and MIS-19 are similar due to similar eccentricity, but those of MIS-5 and MIS-9 are much larger due to larger eccentricity. For the mean summer irradiance and the annual cycle of the mid-month insolation at 65°N, the positive anomaly of MIS-11 which occurred around NHSP is weaker than for MIS-1 and MIS-19 due to a smaller obliquity at that time.

Finally, the time evolution of the total annual irradiation exhibits also a more or less similar pattern for all the interglacials (Fig. 1d). The interglacial $\delta^{18}O$ peaks are preceded by a positive anomaly (relative to today) in the high latitudes of both hemispheres centred over the Poles, lasting more than 10 ka. The differences between the interglacials and today and between the interglacials themselves are mainly in the high latitudes and are very small between 60°N and 60°S. Therefore, in terms of the total energy, the high latitudes are critical regions for explaining the differences between the interglacials. The energy integrated over any time period being only a function of obliquity (Berger et al., 2010) and the obliquity of MIS-1 and MIS-9 being very similar, lead to a similar pattern and amplitude in the annual irradiation for these two interglacials.

4. Results of snapshot simulations with insolation of NHSP

An in-depth analysis of the simulations with insolation of NHSP having been given in Yin and Berger (2012), we focus here mainly on the differences and similarities between MIS-1 and the two groups made of MIS-11 and MIS-19 on one side, and MIS-5 and MIS-9 on the other side.

4.1. MIS-11 and MIS-19 compared to MIS-1

Yin and Berger (2012) showed that, in the framework of the intercomparison of the past nine interglacials, the insolation of MIS-11 contributes to a cooling mainly due to its lower obliquity, but its large GHG-induced warming beats this insolation-induced cooling, making it a warm interglacial only because of its high GHG concentration. MIS-1 and MIS-19 are similar due to their similar GHG concentrations and latitudinal-seasonal distributions of insolation. In response to the combined effect of insolation and CO_2, it is therefore not surprising that MIS-11 and MIS-19 are the closest to MIS-1 among the past nine interglacials. The deviations of these three interglacials from the mean of the nine interglacials look therefore pretty similar (Fig. 2, lower panel), although not for the same reason. The insolation-induced (Fig. 2, upper panel) and GHG-induced (Fig. 2, middle panel) temperatures of MIS-11 differ from MIS-1 and MIS-19, but the differences more or less compensate each other when the combined effect of insolation and GHG is taken into account (Fig. 2, lower panel).

Annually speaking, MIS-1 is similar to MIS-11 and particularly to MIS-19 over most of the Globe (Fig. 3, upper panel). Differences exist in their seasonal temperatures. During boreal summer (JJA) (Fig. 3, middle panel), MIS-11 is slightly cooler than MIS-1 north of ~30°N due to a lower insolation. It is much warmer (by up to 2 °C) over the Southern Ocean due to its higher CO_2 which impact is amplified during austral winter. MIS-19 is slightly warmer than MIS-1 over the majority of the continents related to its slightly larger JJA insolation and the high sensitivity of the continental surface to solar radiation. During boreal winter (DJF) (Fig. 3, lower panel), for MIS-11, its insolation-induced cooling is compensated by its GHG-induced warming and it is slightly warmer than MIS-1 in the mid- and low-latitudes. MIS-19 is not significantly different from MIS-1 over most of the Earth and is only slightly cooler over the Southern Hemisphere (SH) continents. CCSM3 gives similar results except that, in DJF, it simulates an Arctic warmer during MIS-11 than during MIS-1 due to the lack of the summer remnant effect in this model (Herold et al., 2012).

The simulated differences at the regional scale are reflected in proxy records. For example, on one hand, the planktic $\delta^{18}O$ of Hodell et al. (2000) suggests that MIS-11 was not significantly warmer than MIS-1 in the mid-latitudinal South Atlantic (43°S-54°S) although it lasted quite long, and the same happened in the North Atlantic (about 55°N) (McManus et al., 1999). These results are in agreement with the simulations of LOVECLIM (Fig. 3, upper panel) and CCSM3 (Herold et al., 2012), both models showing insignificant warming during MIS-11 over these sites. On the other hand, Bauch et al. (2000) found that MIS-11 was cooler than MIS-1

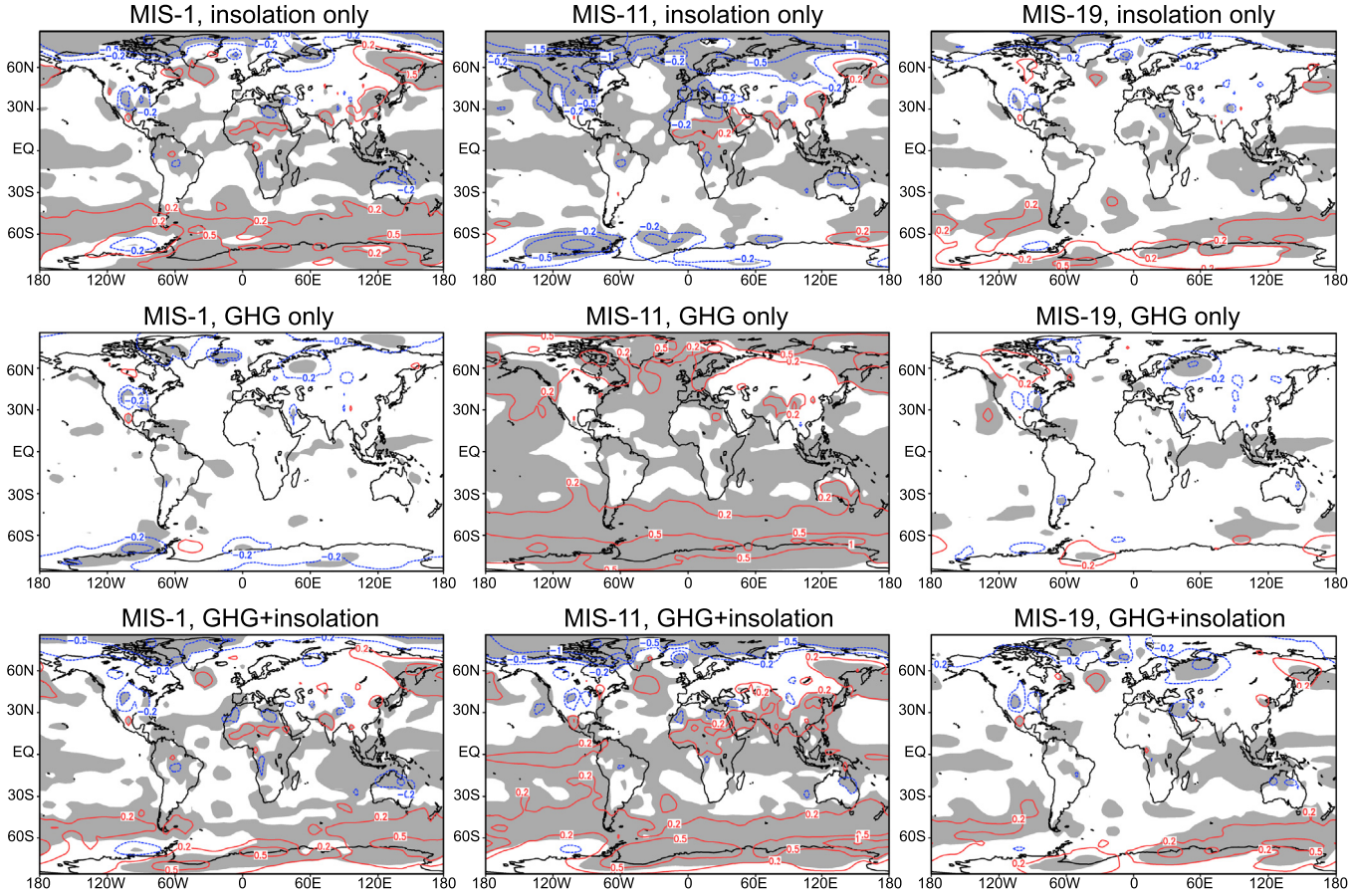

Fig. 2. Annual mean temperature anomalies (°C) during MIS-1, MIS-11 and MIS-19 under the impacts of insolation only, of GHG only and of their combined effect. The anomalies are relative to the reference climate which was simulated with the average GHG and average insolation of the last nine interglacials by Yin and Berger (2012). The first contour line is ±0.2 °C, followed by ±0.5 °C with a contour interval of 0.5 °C. The grey shading shows the 95% confidence level according to a t-test.

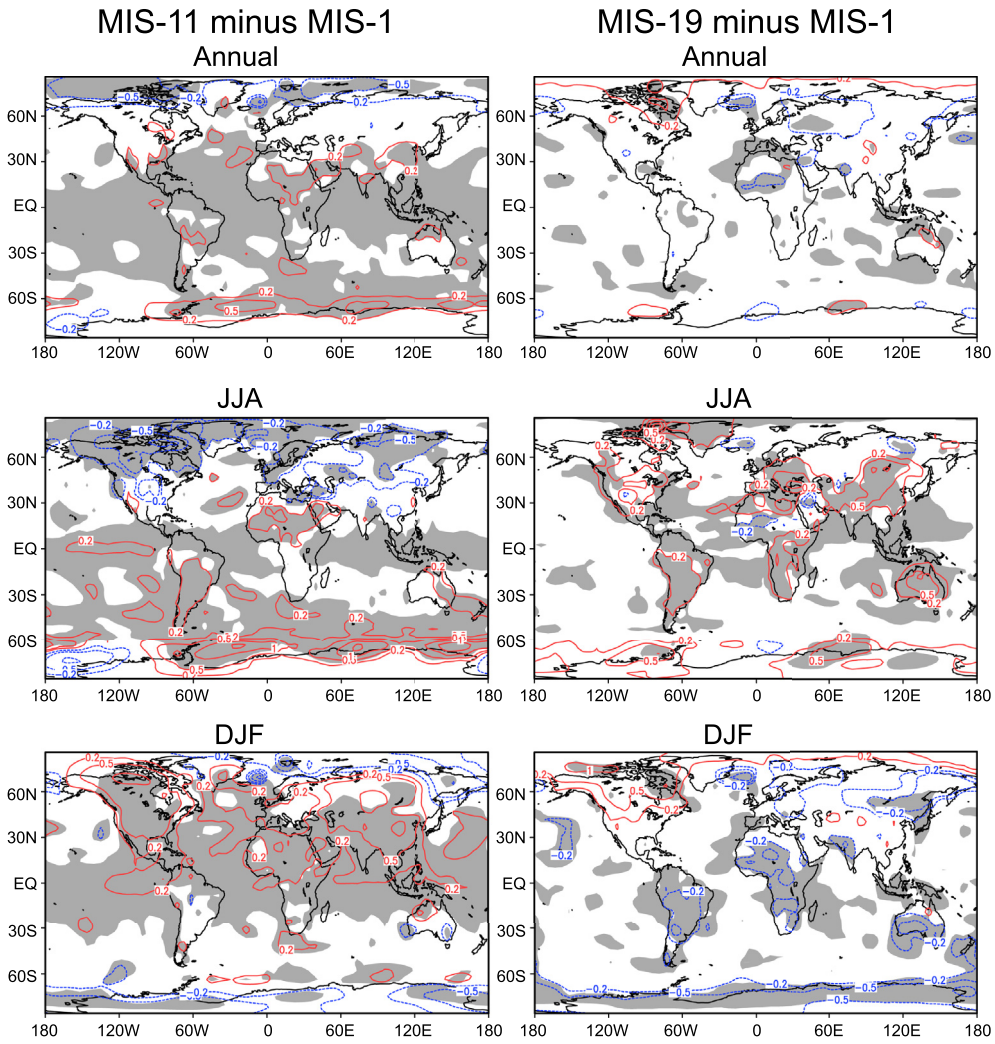

Fig. 3. Differences between MIS-11, MIS-19 and MIS-1 for the annual mean, JJA and DJF surface air temperature (°C) in response to the combined effect of insolation and GHG. The first contour line is ±0.2 °C, followed by ±0.5 °C with a contour interval of 0.5 °C. The grey shading shows the 95% confidence level according to a t-test.

in the Nordic Seas. This is in agreement with the result of LOVECLIM (Fig. 3, upper panel) which simulates a cooling of up to 1 °C in the Nordic Seas during MIS-11 as compared to MIS-1. On the contrary, due to a lack of the summer remnant effect, CCSM3 simulates a warming of up to 1 °C there (Herold et al., 2012). Additionally, Lea et al. (2003) suggested that MIS-11 was almost 1 °C warmer than MIS-1 in the western equatorial Pacific. Such a warming is confirmed by the results of both CCSM3 and LOVECLIM (Fig. 3, upper panel) although it is underestimated by both models. Over the continents, at some locations summarized by Rousseau (2003), MIS-11 was estimated to be similar to or warmer than during the Holocene. Although uncertainties exist in these estimates, they are more or less in line with our model results which show that, annually, MIS-11 is similar to MIS-1 over land in LOVECLIM (Fig. 3, upper panel) and slightly warmer in CCSM3. In both models, the summer over Europe during MIS-11 is cooler than during MIS-1 (Fig. 3, middle panel), which is confirmed by records from Poland (Kukla, 2003).

4.2. MIS-5 and MIS-9 compared to MIS-1

Due to the large difference in the latitudinal and seasonal distribution of insolation, the anomalies of MIS-5 (large eccentricity) and MIS-9 (large obliquity) when compared to MIS-1 are largely different from those of MIS-11 and MIS-19, particularly at the seasonal scale (Fig. 4). During JJA, MIS-5 and MIS-9 are much warmer than MIS-1. The warming over the continents and over the Southern Ocean is the largest reaching more than 5 °C. This JJA warming during MIS-5 and MIS-9 results from a much higher insolation in boreal summer mainly in the high latitudes of the NH. For the Southern Ocean, it is their higher CO_2 concentration and the polar amplification mechanism which explains the large warming. It is however cooler over the tropical band extending from North Africa to East Asia associated with intensified monsoons. This cooling is mainly driven by the ability of the troposphere to radiate away the latent heat released by precipitation and at low level also by the vegetation feedback.

During DJF, the global mean temperature of MIS-5 is lower than MIS-1 and MIS-9. It is cooler by up to 2 °C over the mid-low latitudinal lands as well as over Antarctica (Fig. 4). This is a direct response to its lower DJF insolation which beats the warming effect of its higher CO_2 concentration. However, it is much warmer than MIS-1 over the northern polar regions, resulting from the conjunction of the insolation summer remnant effect (Yin and Berger, 2012) and the CO_2-induced large winter warming. The same large warming happens also during MIS-9. The warming induced by its much larger CO_2 concentration overcomes the cooling induced by its lower DJF insolation in the southern mid to

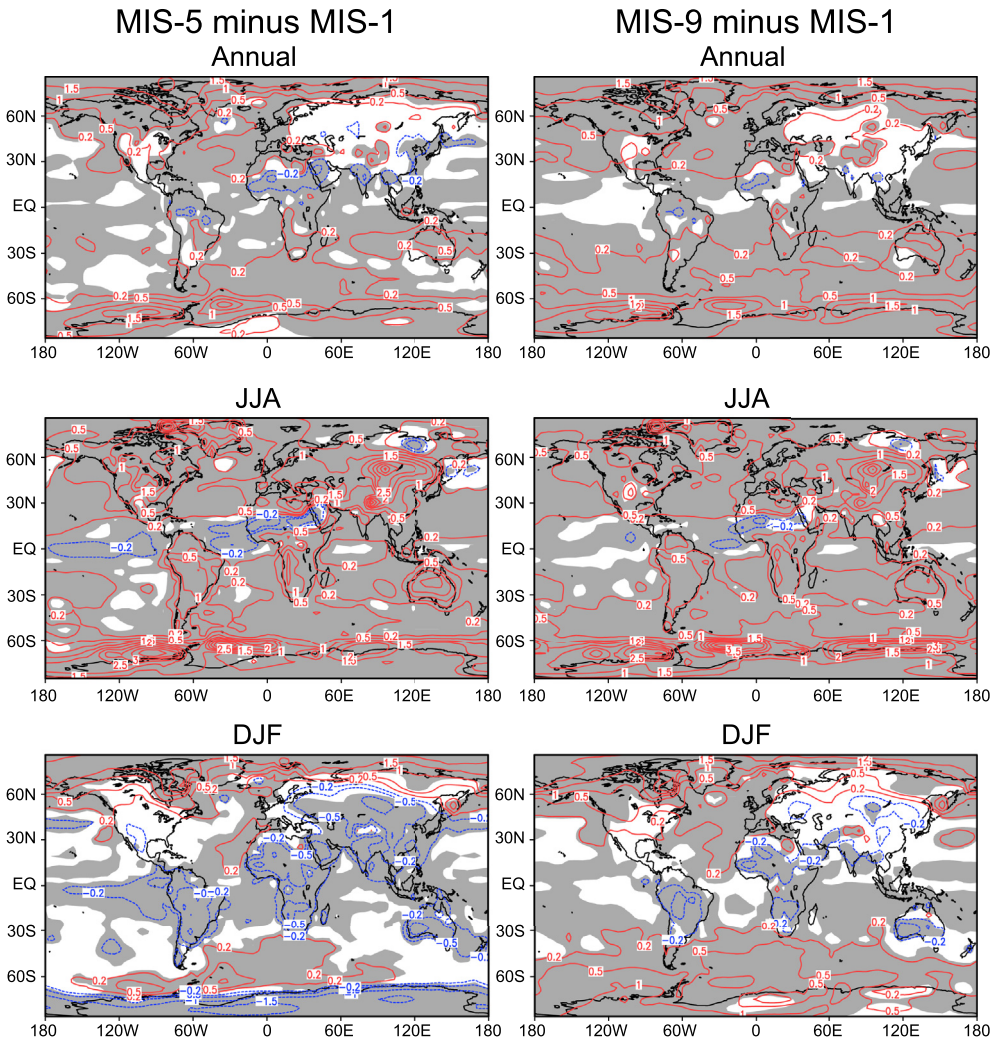

Fig. 4. Same as Fig. 3 except for the differences between MIS-5, MIS-9 and MIS-1.

high latitudes leading to a warming. With a much warmer boreal summer and a cooler boreal winter mainly over the continents, MIS-5 and MIS-9 have a larger NH seasonality. Annually (Fig. 4), MIS-5 and MIS-9 are warmer than MIS-1 over most of the Globe, particularly over the high latitudes. Proxy records (CAPE, 2006) suggest also that MIS-5 is warmer than MIS-1 over much of the northern high latitudes. The temperature record of the EPICA ice core from eastern Antarctica indicates a warming during MIS-5 and MIS-9 of about 4.4 °C and 3.6 °C respectively (Jouzel et al., 2007), a warming which is apparently underestimated by both LOVECLIM (this study) and CCSM3 (Herold et al., 2012).

As already said earlier in this paper, the astronomical forcing during MIS-5 and MIS-9 is largely different from MIS-1 (and the present-day) and their CO_2 concentration is much lower than the anthropogenic CO_2 concentration at present and future, they therefore may not be suitable analogue of the present global warming. However, in terms of climate feedbacks particularly at the high latitudes, there are similarities between the past interglacials and the present anthropogenic warming. First, in both cases, the largest climate change happens at high latitudes of both hemispheres, which involves the positive snow-ice-albedo-temperature feedbacks. For example, the annual Arctic warming during MIS-5 and MIS-9 in Fig. 4 is associated with an annual reduction of 6% in Arctic sea ice area relative to the Holocene Optimum and 20% relative to today. The largest reduction happens during Arctic summer, which reaches 68% relative to today for both MIS-5 and MIS-9. In the Southern Ocean, the annual reduction of sea ice area relative to today is 13% and 19% for MIS-5 and MIS-9, respectively. The reduction in sea ice is accompanied by reductions in snow and albedo in high latitudes, which intensify the warming induced by changes in insolation. Another similarity between the insolation-induced changes during the past interglacials and the CO_2-induced changes at present and future is the asymmetric seasonal response over the polar oceans. Manabe and Stouffer (1980) found that in response to an increase in CO_2 concentration, the warming over the polar oceans is much larger during local winter than during local summer. Similar phenomenon is observed for the interglacial climate in response to an increase in local summer insolation, which has been called “summer remnant effect” by Yin and Berger (2012). In both cases, the energy received in summer is used to melt sea ice, reduce its insulation effect and stored in the upper ocean, and only a small part is to increase the surface air temperature. In winter, the energy is released from the ocean to warm atmosphere. These two similarities shows that, although the main forcings of the past interglacial (insolation) and the present global warming (anthropogenic CO_2) are different, they can lead to the same kind of responses for example in the high latitudes, justifying the use of past warm interglacials as analogues of the

present global warming in terms of climate feedbacks and responses at least for some regions of the world.

5. Simulated climate with the insolation at the interglacial $\delta^{18}O$ peaks

In this section, we discuss the results of the simulations where the insolation at the interglacial $\delta^{18}O$ peaks is used (the second strategy), and compare them with the results of the simulations where the insolation of NHSP is used (the first strategy). Compared to NHSP, the interglacial $\delta^{18}O$ peaks correspond to a time when NH fall occurs at perihelion and obliquity is systematically smaller (Table 1). This leads to less energy received by the whole Earth during boreal spring-summer with the largest depletion at the North Pole, but more energy received during boreal fall-winter with the largest increase over the tropic and subtropics (Fig. 5 for example for MIS-5).

In the simulations where the insolation at the $\delta^{18}O$ peaks of the interglacials is used, in terms of the global annual mean temperature, MIS-9 is still the warmest interglacial followed by MIS-5 (Fig. 6). However, MIS-11 and MIS-19 are cooler than MIS-1 although their CO_{2eq} is 22 ppmv larger than and similar to MIS-1 respectively. The longitude of the perihelion at MIS-11 is about the same as at MIS-1 but its obliquity is one degree smaller. It is shown in Yin and Berger (2012) that when the interglacials have a similar longitude of the perihelion, obliquity plays a dominant role on their astronomically-induced annual mean temperature. Compared to MIS-1, the cooling of MIS-11 is therefore due to its smaller obliquity, a cooling which damps the warming due to its higher CO_2 concentration leading to MIS-11 being finally slightly cooler than MIS-1. MIS-19 is significantly cooler than MIS-1 due to its totally different insolation forcing. Due to their smaller obliquity, MIS-11 and MIS-19 are cooler in the high latitudes of both hemispheres and warmer in the tropics and subtropics, leading to a larger temperature gradient between the low and the high latitudes.

Compared to NHSP (Fig. 6), the climate under the insolation at the interglacial $\delta^{18}O$ peaks is slightly cooler in terms of the global annual mean temperature except for MIS-1 where the opposite seasonal changes tend to cancel each other at the annual scale. At the regional scale, the difference between the two sets of experiments is much larger. The insolation at the interglacial $\delta^{18}O$ peaks leads to much cooler high latitudes in both hemispheres and slightly warmer tropics than the NHSP insolation (see for example MIS-5 in Fig. 7; the other interglacials lead to similar patterns except again for MIS-1). The differences are even larger at the seasonal scale as a direct consequence of the differences in the insolation patterns. During NH spring and summer, the whole Earth is cooler for the insolation forcing at the interglacial $\delta^{18}O$ peaks (figure not shown). During fall and winter, the simulated climate at the $\delta^{18}O$ peaks is warmer than the NHSP one except in high NH polar latitudes, a direct consequence of the summer remnant effect. As far as the analogues are concerned, different from the conclusions when NHSP insolation is used, no analogue of MIS-1 can be found when insolation at the interglacial $\delta^{18}O$ peaks is used.

Given the obvious differences induced by different insolation forcing, comparing model results to proxy data might in some way help to see which insolation is better in simulating the interglacial Optima. Turney and Jones (2010) made a compilation of the annual mean surface air temperature and sea-surface temperature for the Last Interglacial. They averaged the temperature estimates across the isotopic plateau in the marine and ice records and the period of maximum warmth in terrestrial records. It is known that this reconstruction is not perfect, at least due to the resolution in the chronology and to the climatic interpretation of the proxies, but it provides a first-order estimate of the global climate for the Last Interglacial Optimum and has been used in the PMIP data-model comparison (Lunt et al., 2013). It is used here to compare with the results of both the NHSP and the $\delta^{18}O$ peaks simulations. It is acknowledged that, given the biases in climate models themselves and in the climate forcing selection, as well as uncertainties in the proxy reconstructions, it should be cautious to draw definite conclusions from such model-data intercomparison. However, our purpose here is to see which insolation leads to a result which is the closest to the proxy reconstructions. Fig. 7 shows that both simulations of MIS-5 are warmer than Pre-Industrial time in the mid-high latitudes and cooler in the low latitudes, in agreement with proxy reconstructions. When compared with proxy data, the amplitude of cooling in low latitudes and warming in high latitudes is better represented by the NHSP simulation. This confirms that the insolation when NH

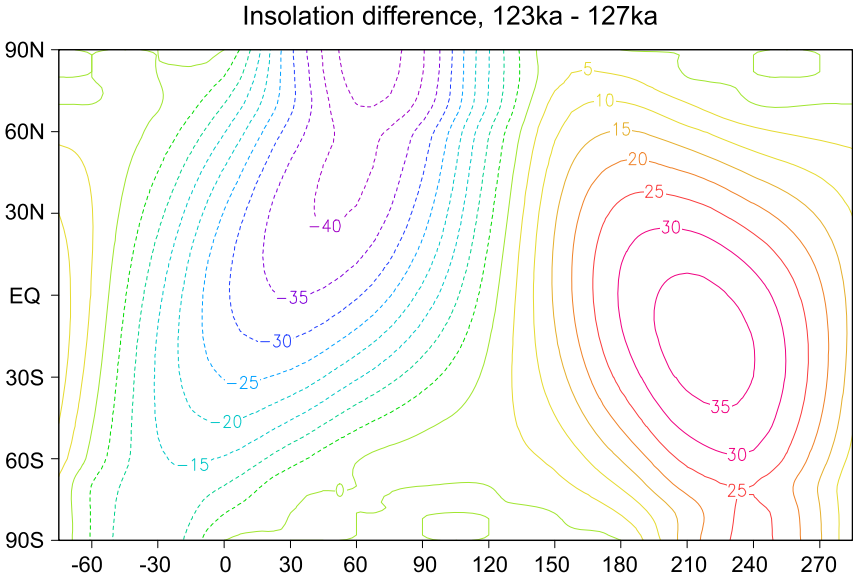

Fig. 5. Difference in latitudinal-seasonal insolation (Wm^{-2}) distribution between the date of the marine $\delta^{18}O$ peak (123 ka BP) and that when NH summer occurs at perihelion (127 ka BP) for MIS-5. Label on the X-axis indicates the true longitude of the Sun from the beginning to the end of the year (0° and 180° are for the spring and fall equinoxes; 90° and 270° are for the summer and winter solstices). Insolation is calculated from the long-term variations of eccentricity, precession and obliquity (Berger, 1978).

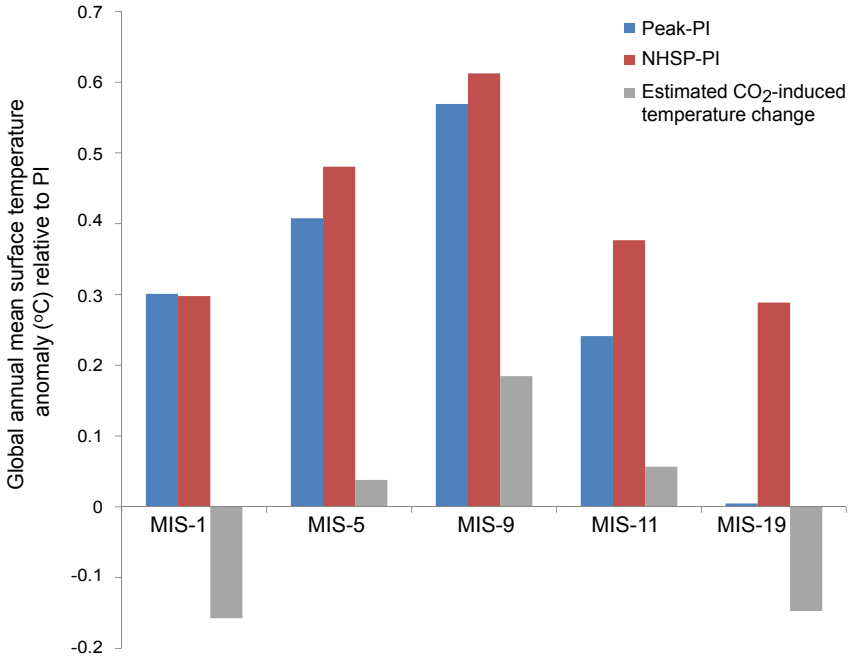

Fig. 6. Simulated global annual mean temperature anomalies (°C) (relative to the Pre-Industrial time) of the five interglacials. Red bar is for the snapshot simulations where insolation of NHSP is used and blue bar is for those where insolation at the interglacial $\delta^{18}O$ peak is used. Grey bar indicates the CO_2-induced temperature change which is estimated based on the climate sensitivity of LOVECLIM.

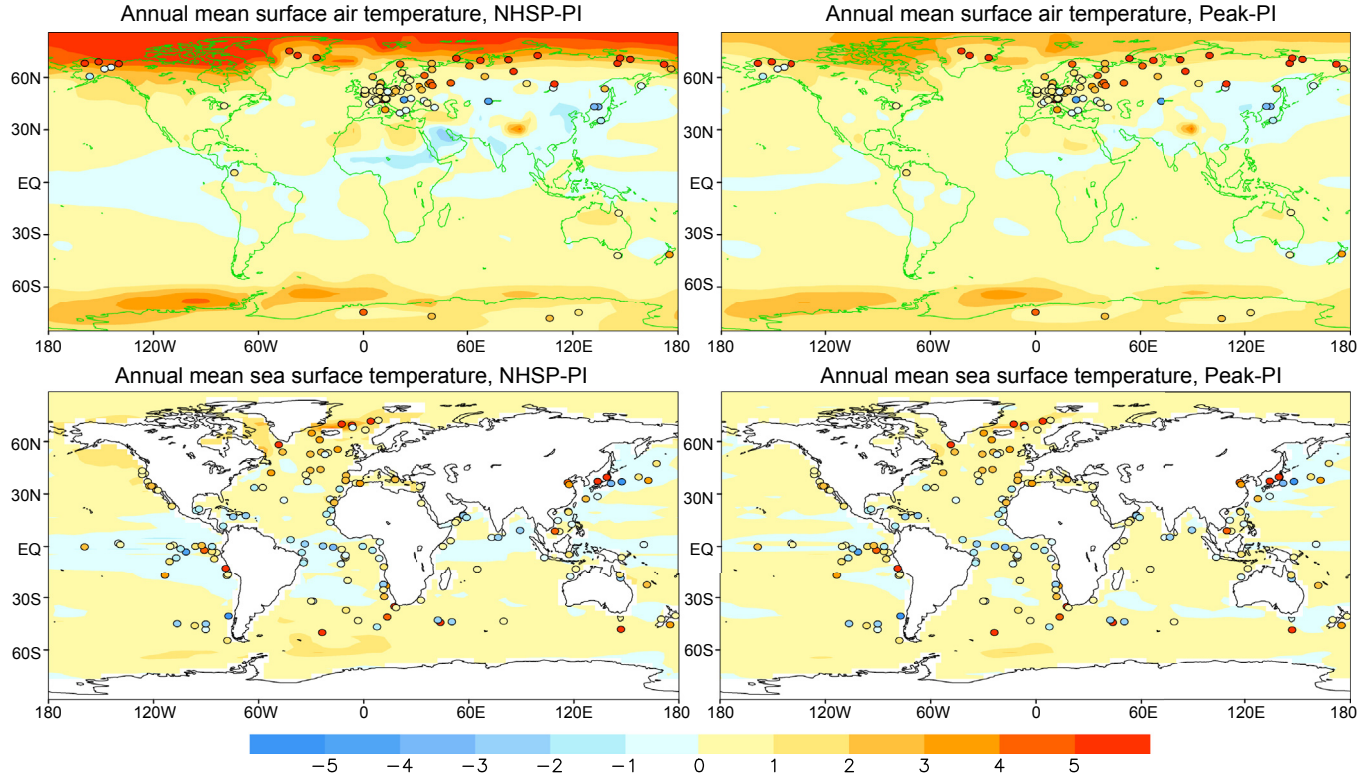

Fig. 7. Differences (°C) between MIS-5 and Pre-Industrial in annual mean surface air temperature and sea surface temperature. The results of the NHSP simulation are on the left, and those of the interglacial $\delta^{18}O$ peak simulation are on the right. The dots denote the compilation of proxy records by Turney and Jones (2010).

summer occurred at perihelion is a better choice than the insolation at the interglacial $\delta^{18}O$ peaks when attempting to reproduce the interglacial climate Optimum reconstructed from proxy records.

6. Transient climate response to insolation only

Given the importance of insolation in the discussion of the analogues, transient simulations with varying astronomical

configurations (the third strategy) appear to be particularly important. In this section, we discuss the results of the transient simulations where CO_2 is kept constant (280 ppmv) with time, which allow to investigate the climate response to insolation only. Although the periods of the transient simulations are centred over interglacials, they cover almost the full range of variations of each astronomical parameter. Therefore, the results discussed here can be considered as being valid not only for the interglacial conditions but also as an indication of the climate response to the astronomical forcing in general, being kept in mind however that the CO_2 and ice sheets are prescribed to their PI values.

Based on the results of nine snapshot experiments, Yin and Berger (2012) found that the global annual mean temperature is highly correlated with obliquity. The transient simulations of the five interglacials cover a much larger range of obliquity and precession, and provide therefore more information about the relationship between temperature and the astronomical parameters. Fig. 8a shows that the global annual mean temperature of the five transient simulations is also highly correlated with obliquity, but the modulation by precession is obvious. For a given obliquity, two different temperature values can exist due to difference in precession. Individual linear regressions (Fig. 8a and b) confirm the dominance of obliquity in the global annual mean temperature, which alone explains 85% of the variance. An increase of 1° in obliquity leads to an increase of 0.38 °C in the global annual mean temperature (Fig. 8a). In order to quantify the relative weight of each astronomical parameter on the global annual mean temperature, a multiple linear regression analysis is performed. Such a regression (using the standardized values of the variables) shows that 91% of the variance of the global annual mean temperature can be explained by the combination of the three astronomical parameters with obliquity dominating (Table 2). Based on the regression analysis, an equation showing the relationship between the variations of temperature and the three astronomical parameters can be given as:

$$T = 0.76obliquity - 0.29precession + 0.04eccentricity \quad (1)$$

In Equation (1), the standardized values of all variables are used. T denotes global annual mean temperature. According to Equation (1), an OPE (obliquity-precession-eccentricity) index which equals to the right side of Equation (1) can be created to estimate the global climate sensitivity to the astronomical parameters. This index is similar to the ETP index of Imbrie and Imbrie (1979), but here the relative weight of the parameters is taken into account. Over the selected time intervals of the five interglacials, the OPE index varies between about −2 and 1.5 and its increase by 1 leads to an increase of 0.26 °C in global annual mean temperature (Fig. 8c). Its minimum corresponds to a minimum of obliquity and a maximum of precession (which means NH summer occurring at aphelion). Fig. 8c shows that the outliers occur close to the minimum of the OPE index which corresponds to the period from 113 to 116 ka BP of the MIS-5 simulation. During this time interval, the coinciding obliquity minimum and precession maximum (Fig. 9) leads to very low insolation in the NH. Regional analysis shows that these outliers result from the climate response in the northern mid and high latitudes which are the most sensitive to insolation change due to the existence of large continental area and the positive feedbacks between temperature and the albedo of snow and sea-ice. These outliers illustrates the non-linearity of the relationship between climate and the astronomical parameters when extreme astronomical conditions occur, which effect is amplified by internal climate feedbacks.

The multiple regression analysis at the regional scale shows also that most of the variations of the annual mean temperature in the mid and high latitudes can be explained by the combination of precession, obliquity and eccentricity but not the low latitudes between 30°N and 30°S (see R^2 in Table 2). Obliquity has a larger control over the southern high latitudes than over the northern ones, and the influence of precession becomes more important in the NH. This is in agreement with the results of the snapshot simulations discussed in Yin and Berger (2012). For the low latitudes, only a small part of the annual mean temperature variation can be explained by the combination of obliquity, precession and eccentricity. This might be due to the small variation of the irradiation over these regions (Berger et al., 2010) which leads to the increasing importance of internal feedbacks, such as those related to monsoon. In parallel, Fig. 9 shows that the variation of the annual mean temperature of the NH low latitudes is characterized by a frequency higher than in other latitudinal zones, a result similar to the sub-precessional signal found by Berger et al. (2006).

Fig. 9 shows that the variations of the annual mean temperature of different regions are far from being in phase. One of the reasons is related to the phase relationship between precession and obliquity which have a different weight on the annual temperature of different latitudes (Table 2). MIS-11 offers the best illustration, because its precession minimum and obliquity maximum are almost in anti-phase (Fig. 9). The obliquity maximum precedes the precession minimum by 8 ka, a lag which allows a better discrimination between their respective impacts. For the annual mean temperature (Fig. 9, MIS-11), the maximum response in the southern mid and high latitudes is more or less stationary lasting from about 420 to 410 ka BP, whereas the maximum in the NH mid and high latitudes is sharper, centred at 411 ka BP and lasting only a few thousands of years. The southern maximum occurs earlier than

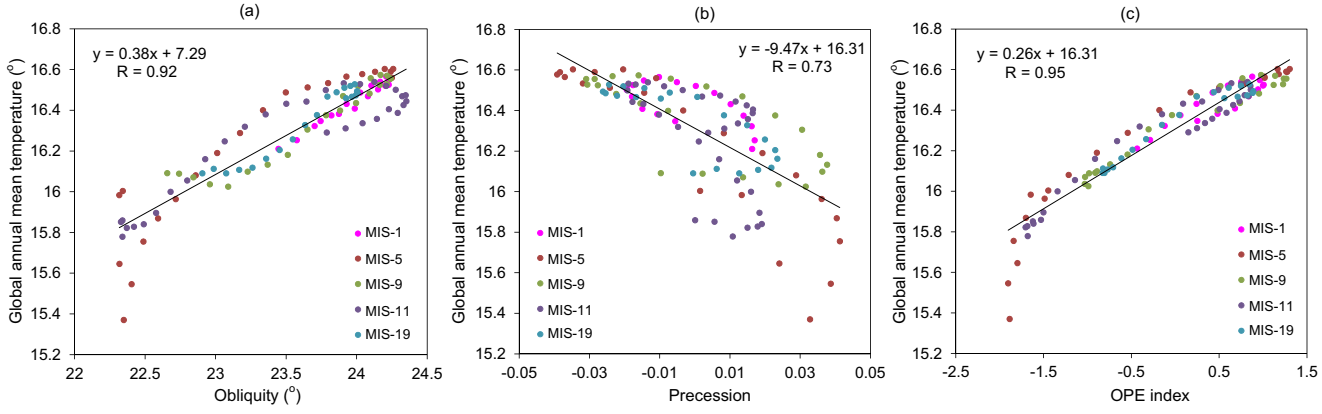

Fig. 8. Linear regressions between global annual mean temperature (°C) and obliquity (°) (a), and precession (b), and OPE index (c). The temperature data are the 1000-year averages of the transient simulations where CO2 is fixed to 280 ppmv. The astronomical parameters are from Berger (1978).

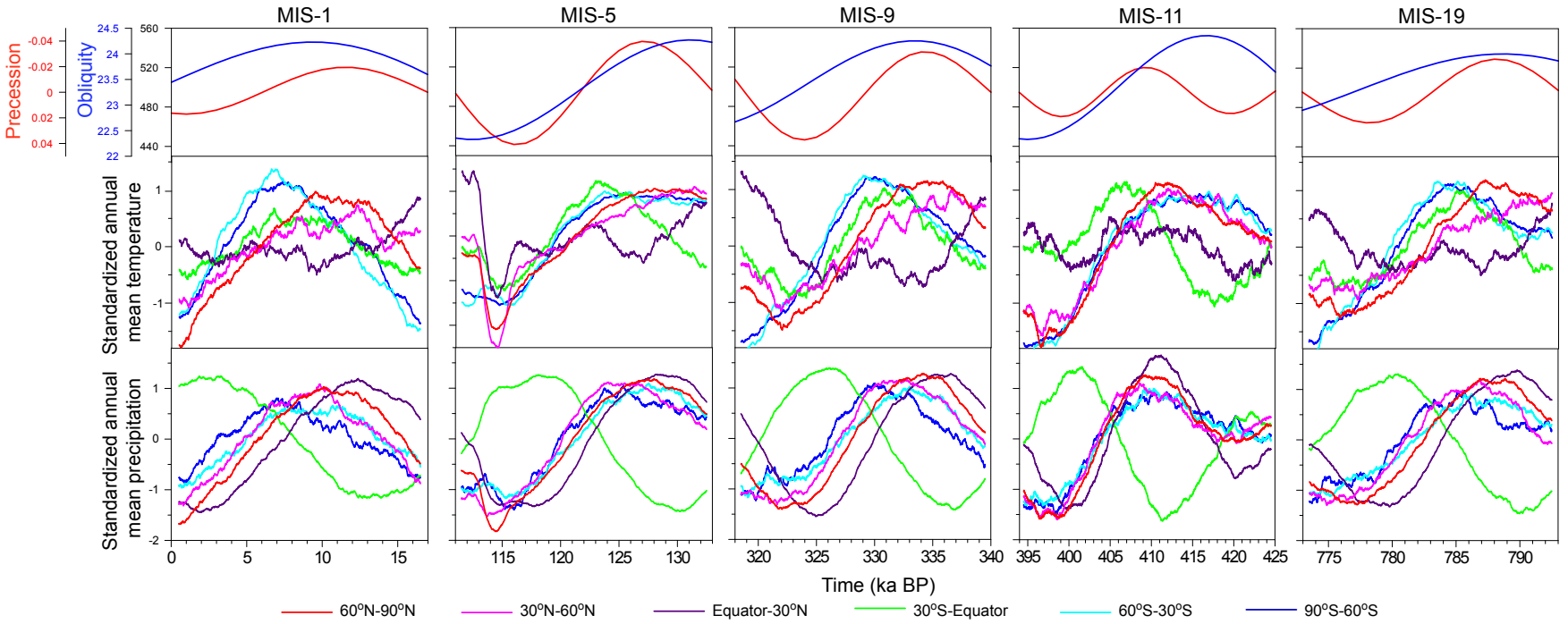

Fig. 9. Upper panel: Obliquity (°) and precession over the periods of transient simulations for MIS-1, MIS-5, MIS-9, MIS-11 and MIS-19; Middle panel: standardized annual mean temperature of different latitudinal zones; Lower panel: standardized annual mean precipitation of different latitudinal zones. The temperature and precipitation data are from the transient simulations where CO_2 concentration is fixed to 280 ppmv. The 1000-year running mean of standardized temperature and precipitation is plotted.

Table 2
Percentage of climate variance explained by the combination of obliquity, precession and eccentricity (R^2) and regression coefficients of linear multiple regression between simulated climate variables (the predictand) and the three astronomical parameters (the predictors). The results of the five transient simulations with time-varying insolation but constant GHG concentration are used, which allows to have the impact of insolation alone.

		Global	90°S–60°S	60°S–30°S	30°S-Equator	Equator-30°N	30°N–60°N	60°N–90°N
Annual mean temperature	R^2	0.91	0.89	0.84	0.36	0.19	0.79	0.94
	Obliquity	0.76	0.96	0.97	−0.21	−0.47	0.68	0.63
	Precession	−0.29	−0.01	0.08	−0.63	−0.46	−0.31	−0.46
	Eccentricity	0.04	0.13	0.14	0.13	−0.32	−0.01	0
Annual mean precipitation	R^2	0.91	0.78	0.92	0.84	0.97	0.78	0.94
	Obliquity	0.35	0.77	0.66	−0.1	0.1	0.58	0.47
	Precession	−0.72	−0.17	−0.39	0.84	−0.92	−0.41	−0.63
	Eccentricity	0.13	0.36	0.41	0.06	0.01	0.08	0.06
JJA surface temperature	R^2	0.99	0.97	0.77	0.98	0.94	0.98	0.97
	Obliquity	0.26	0.48	0.79	−0.21	−0.12	0.27	0.48
	Precession	−0.82	−0.65	−0.18	−1.09	−1.03	−0.81	−0.61
	Eccentricity	0	0.14	0.17	0.01	−0.09	−0.01	−0.08

the northern one as a response to the obliquity maximum, the maximum in the northern mid and high latitudes being modulated by precession and occurring a few thousands of years later.

Opposite to MIS-11, during MIS-19 and MIS-9, precession minimum and obliquity maximum are in phase. The annual mean temperature maxima of different regions remain nevertheless far from being in phase (Fig. 9), which reflects the role of the internal feedbacks of the climate system more than that of the phase relationship between precession and obliquity. During MIS-9 and MIS-19, the annual mean temperature maxima in the NH mid and high latitudes are in phase with precession minima (or June solstice NH insolation maxima) but precede the temperature maxima of the SH mid and high latitudes by about 5 ka. Similar features appear also during MIS-1 where the obliquity maximum lags the precession minimum by only 3 ka. The results of MIS-1, MIS-9 and MIS-19 show that when precession minimum and obliquity maximum are in phase, the temperature of NH mid-high latitudes leads the SH ones, indicating a higher sensitivity of the NH climate to insolation change, which results from the fundamental difference between the proportions of continental and oceanic expanses in the two hemispheres. During MIS-5, obliquity maximum precedes the precession minimum, like during MIS-11, but only by 4 ka. Due to the response time of the vast Southern Ocean, the temperature maxima in the SH and NH mid and high latitudes are more or less in phase, preceding the SH tropical maxima (which is controlled by precession, see Table 2) by about 5 ka (Fig. 9). In summary, as far as the phase relationship between the annual mean temperatures of different regions is concerned, MIS-1 is similar to MIS-9 and MIS-19 but different from MIS-11 and MIS-5. Due to the similarity in the amplitude of obliquity, the annual mean temperature of the global Earth and of the SH mid-high latitudes of MIS-1 and MIS-9 are quite similar.

Different from the global annual mean temperature which is highly correlated with obliquity, the global annual mean precipitation is highly correlated with precession (Table 2). Linear multiple regression analysis (Table 2) shows that most of the variations of the annual mean precipitation of different latitudinal zones can be explained by the combination of obliquity, precession and eccentricity but with different weight of the three parameters at different latitudinal zones. The precipitation at low latitudes is exclusively controlled by precession, with northern one and southern one being anti-phase. Such an anti-phase relationship has also been observed in spelaeothem records (Wang et al., 2004) and is related to the seasonal migration of the Intertropical Convergence Zone. For the precipitation of mid-high latitudes of both hemispheres, obliquity also play important role (Table 2). Dominated by different astronomical parameters, the variations of precipitation in different latitudinal zones are not necessarily in phase (Fig. 9).

Although different latitudinal zones have different variations in annual mean temperature and precipitation, examination of the seasonal behaviour of the interglacial climate shows that they share one common feature: the variations in the JJA temperature of different zones (except the Southern Oceans) are all in phase with each other and are dominated by precession (Fig. 10, Table 2), their maxima occurring when NH summer occurs at perihelion. Unlike the other regions, the JJA air temperature over the Southern Oceans (between 30°S and 60°S) during MIS-1, -5, -9 and -19 does not reach its maximum when NH summer occurs at perihelion (it lags behind by around 4 ka). This is because when NH summer occurs at perihelion, the SH summer (DJF) occurs at aphelion and the SH summer insolation as well as the SH summer temperature over the Southern Oceans reach their minima, which effect is transferred to the local winter (JJA) through the summer remnant effect preventing the occurrence of a JJA temperature maximum there. MIS-11 is however an exception due to the almost anti-phase between obliquity and precession. When NH summer (JJA) occurs at perihelion (at 409 ka BP), its air temperature over the Southern Oceans during local summer (DJF) fails indeed to reach a minimum, because it is still under the influence of the maximum which occurred at 420 ka BP when the obliquity maximum falls almost in phase with SH summer at perihelion. This leads to only a weak cooling impact of the local summer climate on the local winter one (JJA), so that the local JJA temperature maximum occurs when NH summer is at perihelion (Fig. 10). This behaviour probably contributes, at least partly, to the exceptional length of MIS-11 (see Section 7). The exceptional phase relationship between obliquity and precession during MIS-11 could also explain the simulated simultaneous occurrence of warm winters and warm summers in the Arctic 409 ka ago, whereas during the other interglacials winter warming lags behind summer warming by a few thousands of years. Such occurrence, with at the same time, the appearance of a warm winter and a moderately cool summer over Antarctica and its surrounding oceans might be at the origin of ice sheet melting and a particularly large sea-level rise during MIS-11 as suggested by some proxy studies.

The common feature of different latitudinal zones implies that JJA temperature is the broadest common representative characteristic of the different regions for different interglacials and might therefore be used easily and more confidently in the intercomparison between the interglacials and between regions. In addition, as JJA temperature is anti-phase with precession (Table 2) (it means in phase with insolation), its maximum response happens when NH summer occurs at perihelion, the response at the dates of the interglacial $\delta^{18}O$ peaks being smaller. This gives another credit to using the insolation of NHSP to simulate the climate Optimum of

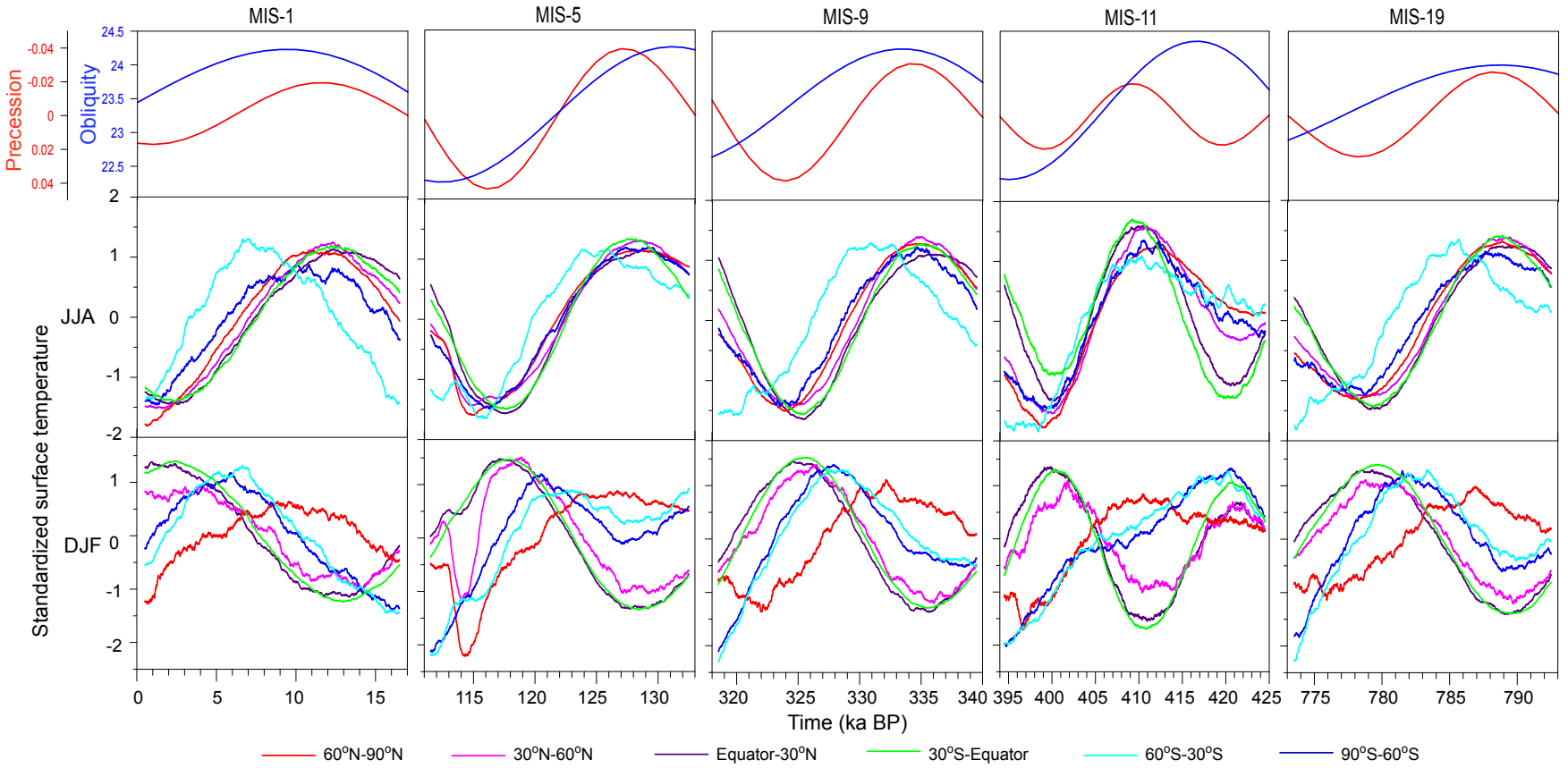

Fig. 10. Same as Fig. 9 except that the middle panel and lower panel are for JJA and DJF surface temperature, respectively.

the interglacials when snapshot experiments are used (as in Yin and Berger, 2012). JJA temperature might not be the ultimate product of the climate system which can be used to best define and compare the interglacials between them together. Another excellent product, at least at the global scale, is the global ice volume and the related eustatic sea level. The climate-ice sheet coupled model CLIMBER by Ganopolski and Calov (2011) provides such information on the simulated NH ice sheets of the last 800 ka. The interglacial peaks pinpointed in their simulated NH ice volume have no constant phase relationship with obliquity, but do have one with precession. They lag behind precession minimum or NH June solstice insolation maximum by a few thousands of years coherently in all the five interglacials. In parallel, the global sea level compilation of the Last Interglacial by Kopp et al. (2009) shows that the highest sea level happened also a few thousands of years after the June solstice NH insolation maximum. The lag between ice volume/sea level and NH summer insolation reflects the response time of the slow processes related to ice sheets and confirms the conclusion of Kukla et al. (1981) that the interglacials are associated with maximum NH summer insolation.

The varying phasing of the temperature and precipitation between different regions and between them and precession/obliquity/insolation means that one must be cautious when astronomically tuning the time scale of a proxy or tuning it to another proxy. The maximum in a proxy does not coincide necessarily with the maximum in a proxy from other regions or with the maximum insolation forcing. Our modelling results suggest however that it is not the case for the proxies of JJA temperature which could be well compared between them together as they are in phase with precession for different regions and therefore could be used more confidently in the tuning procedure.

In the analysis of seasonal results of paleoclimate simulations, one difficulty is related to the choice of seasons calculation (astronomical or calendar) (Joussaume and Braconnot, 1997). The length of the seasons, which are astronomically defined, varies indeed with time (Berger and Loutre, 1994). This implies that some days of the calendar seasons traditionally used in paleoclimate modelling (eg. DJF, JJA, …) are not belonging to the same astronomical season from one time to another. Whereas at the present-day spring and summer are the longest seasons (with 93 and 94 days against 90 and 89 for fall and winter), this is not the case most of the time during the interglacials, in particular around the maxima of the global annual mean temperature. At these times, the length of fall and winter together varies between 6.2 (during MIS-1) and 11.9 (during MIS-5) days longer than at present, and the boreal winter solstice falls between December 14.6 (during MIS-9) and 19.9 (during MIS-11) against 22.2 at today. According to some recent studies (eg. Timm et al., 2008; Chen et al., 2011), the calendar effect could cause a phase shift on temperature and precipitation during boreal autumn (September-October-November), but the other seasons are not critically biased. We therefore assume that our conclusions related to the JJA and DJF temperature are not altered by the use of calendar days.

7. Analogues of the entire Holocene and of its natural near future

The idea of searching for analogues is to expect finding in the past something similar to the future climate which will result from either natural or anthropogenic impact. It will also allow setting our present climate back in the context of the past interglacials. As explained in Section 1, since the present-day CO_2 concentration and its projected future under human influence have no analogue over the last one million years, it was decided to compare the past interglacial climates with the “natural” climate of the Holocene, of the present-day and its near future.

When discussing the natural climate of the Holocene (MIS-1), it is unavoidable to mention the debate about the origin of the increase in CO_2 and CH_4 during the late Holocene. Based on the observation that the concentration of CO_2 and CH_4 did not rise at the end of the four interglacials prior to the Holocene, Ruddiman (2007) hypothesizes that the rise of CO_2 and CH_4 between 7ka BP and Industrial Era is not of natural origin but associated with early human interventions. Many studies have tested this hypothesis, some confirming and some not (see a review in IPCC report 2013, chapter 6). In particular, recent modelling results show that the 20 ppmv increase in the CO_2 concentration during the late Holocene is most probably related to ocean processes and does not require anthropogenic forcing (Kleinen et al., 2010). This is why we used the concentration of CO_2 and CH_4 reconstructed from the EPICA ice cores (Luthi et al., 2008, Fig. 11) in our Holocene transient simulation. If Ruddiman's hypothesis is right, caution should be taken in the comparison between the past interglacials and the most recent millennia of Holocene. However, whatever it is right or not, an increase of 20 ppmv in CO_2 during the late Holocene remains much smaller than the increase of 120 ppmv above the 280 ppmv pre-industrial value during the 20th and 21st centuries and even much smaller than the increase of hundreds of ppmv in the IPCC scenarios for the future due to human activity. We might therefore assume that the late Holocene climate is sufficiently close to a “natural” one when compared to the present global warming caused by much larger anthropogenic CO_2 increase.

The PI climate is considered here as the natural climate for the present-day and for the next centuries, because of the slow variations in the Earth's astronomical parameters and insolation, but assuming 280 ppmv for the atmospheric CO_2 concentration. Comparing the PI climate to the climate of the elapsed Holocene and of the other interglacials helps to locate the present and the near future natural climate in the context of the warm interglacials and provides the background on which the impact of human activities can be tested.

As far as the snapshot simulations are concerned, all simulations of the five interglacials of Sections 4 and 5 show a global annual climate warmer than PI (Fig. 6), except for the MIS-19 $\delta^{18}O$ peak simulation. This similarity between the climate of MIS-19 at its $\delta^{18}O$ peak and of the PI climate extends to the regional scale and to precipitation. This suggests that MIS-19 climate at its $\delta^{18}O$ peak might be taken as an analogue for the natural present-day climate and its future. It underlines the necessity of obtaining more proxy-based climate reconstructions of high temporal resolution during MIS-19. In order to estimate the individual contributions of insolation and CO_2 to the interglacial climate, Yin and Berger (2012) used the factor separation analysis. The CO_2-induced change in the global annual mean temperature can also be estimated from the climate sensitivity of LOVECLIM (1.9 °C for a doubling of CO_2 concentration at PI time). This is only a first-order estimation, because the climate sensitivity was shown to depend on the astronomical configurations and the background climate and therefore varies from one interglacial to another (Yin and Berger, 2012). Fig. 6 shows that, as expected, the lower CO_2 of MIS-1 and MIS-19 leads to a slight cooling, and the higher CO_2 concentration of the other three interglacials leads to a slight warming. However, it must be stressed that a large part of the warming relative to PI of all the interglacials is mainly caused by change in insolation (whatever insolation is taken at the $\delta^{18}O$ peak or for NHSP), a situation totally different from the present-day global warming which is mainly caused by the anthropogenic CO_2 increase.

As far as the transient simulations are concerned, under the influence of insolation alone, the simulated past interglacials are

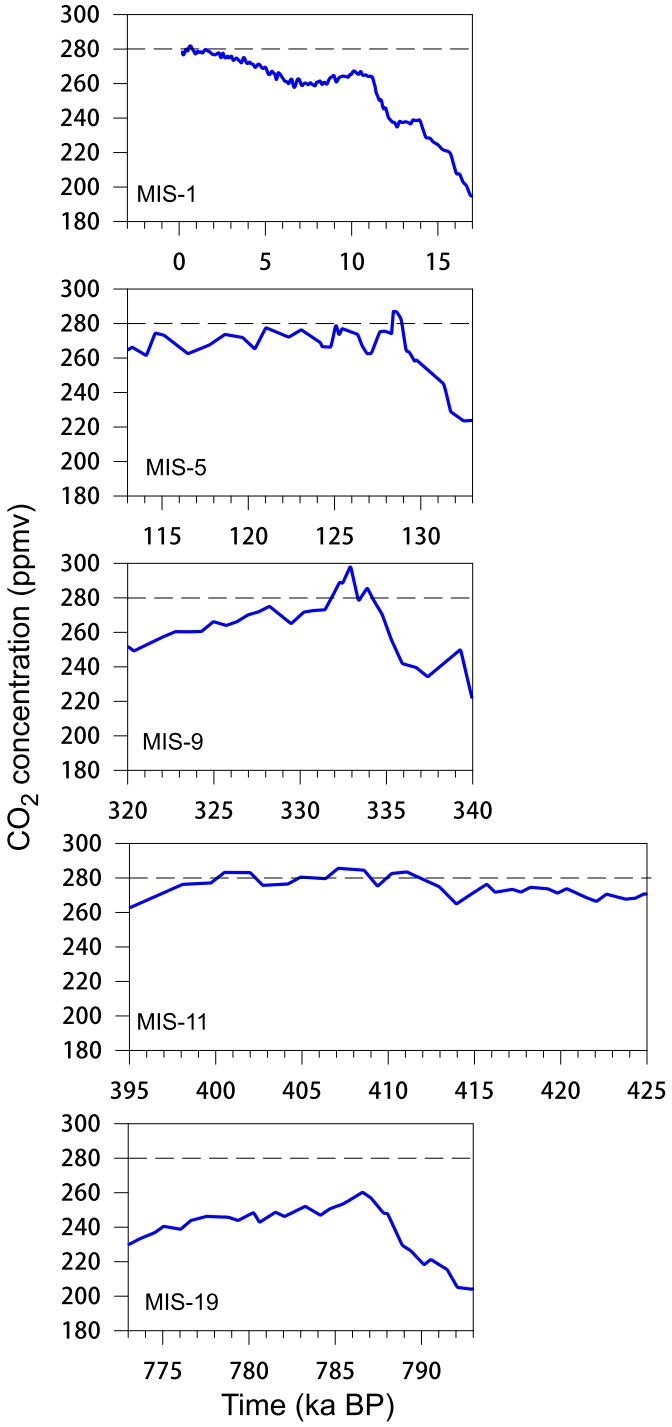

Fig. 11. CO_2 concentration (ppmv) used in the second set of transient simulations with time-dependent CO_2. Horozontal dashed line indicates the CO_2 level of PI which is 280 ppmv. Data are from Luthi et al. (2008).

shown to be warmer than PI in JJA, slightly warmer at the annual scale but cooler in DJF (Fig. 12a). This can be explained by the relatively small obliquity at pre-industrial time and its NH summer occurring at aphelion. Therefore, the past interglacials receive more energy than PI in the NH from April to July over a period of more than 10 ka (Fig. 1c). The relatively small eccentricity of PI also contributes to reduce its seasonal contrast. When compared to the entire MIS-1 (including the elapsed part and the next 3 ka, dashed lines in Fig. 12a), the global annual mean temperature of MIS-9 is the closest to MIS-1 due to their similar obliquity which drives the annual irradiation (Fig. 1d) and dominates the variation of global annual mean temperature. In terms of seasonal temperature (Fig. 12a), MIS-19 is the closest to MIS-1, followed by MIS-11, as reflected also in the time evolution of daily insolation (Fig. 1b and c). Due to the larger variation in the time evolution of daily insolation resulting mainly from a large eccentricity, the amplitude of the seasonal temperature variation is larger during MIS-5 and MIS-9, these two interglacials being warmer than MIS-1 during boreal summer and cooler during boreal winter (Fig. 12a).

From CO_2 concentration point of view, it is lower than the PI level (280 ppmv) during almost all the intervals of the transient simulations except at the overshoots of MIS-5 and MIS-9 and over a 10-ka long plateau during MIS-11 (Fig. 11). If the Ruddiman's hypothesis (Ruddiman, 2007) is true, MIS-19 would be a good analogue of MIS-1 in respect of both the time evolution and the amplitude of CO_2 concentration. By comparing Fig. 12b to a, one can see that the main structure of the temperature evolution during the past interglacials is dominated by change in insolation, and it is only slightly modulated by change in CO_2 concentration. Obvious CO_2-induced cooling in the seasonal and annual mean temperatures is mainly observed during the deglacial time before the peaks of MIS-1, MIS-5, MIS-9 and MIS-19 due to a much lower CO_2 concentration. These results show that, unlike the present global warming which is caused by anthropogenic CO_2 increase, the major factor controlling the interglacial climate change is insolation, in line with the statement of Ganopolski and Robinson (2011).

Under the combined effect of insolation and CO_2, during JJA, the warmer-than-PI temperature lasts 14 ka, 12 ka, 12 ka, more than 20 ka and 10 ka for MIS-1, -5, -9, -11 and -19 respectively. Given the importance of JJA temperature on northern hemisphere ice sheet dynamics, such a long lasting JJA warming during these interglacials might have contributed to the melting of the ice sheets. For the annual mean temperature, the length of the warmer-than-PI periods becomes 10 ka, 8 ka, 8 ka, 20 ka and 1 ka for MIS-1, -5, -9, -11 and -19 respectively. The start and end of the warmer-than-PI intervals compare fairly well with the intervals during which the marine $\delta^{18}O$ remains low (which means warm condition). The lower CO_2 concentration during MIS-19 shortens significantly the interval of warm annual mean temperature (Fig. 12b), but does not influence much the duration of its warm JJA temperature. Although MIS-19 seems to be an even better insolation analogue of MIS-1 than MIS-11 (see Section 3), it appears much shorter than MIS-11 in many different proxy records. This can be explained by its lower CO_2 concentration (which is opposite of what has happened during MIS-11). It remains however that MIS-19 is still a good analogue of MIS-1 when the influence of CO_2 is additionally taken into account (Fig. 12b). The warm interval of MIS-11 is the longest and its seasonal contrast is the smallest, which confirms the long duration of MIS-11 found in earlier studies (eg. Berger and Loutre, 2002, 2003; Droxler et al., 2003). This exceptional duration of MIS-11 is related to its long-lasting low eccentricity and high CO_2 concentration. Sensitivity analyses have indeed shown that the existence of a CO_2 concentration which remains high during the decreasing phase of insolation around 400 ka BP played a role in the long duration of MIS-11. This exceptional length of MIS-11 is also related to the anti-phase relationship between obliquity maximum and precession minimum which effects compensate each other, contributing to sustain a long moderately warm interval. Although th warmth intensity of MIS-11 is not large as compared to some other interglacials like MIS-5, the long duration of MIS-11 could have played an important role in the ice sheet melting and sea level rise, such exceptional features having been suggested by proxy records (eg. de Vernal and Hilaire-Marcel, 2008; Olson and Hearty, 2009; Raymo and Mitrovica, 2012). Anyway, due to its long lasting

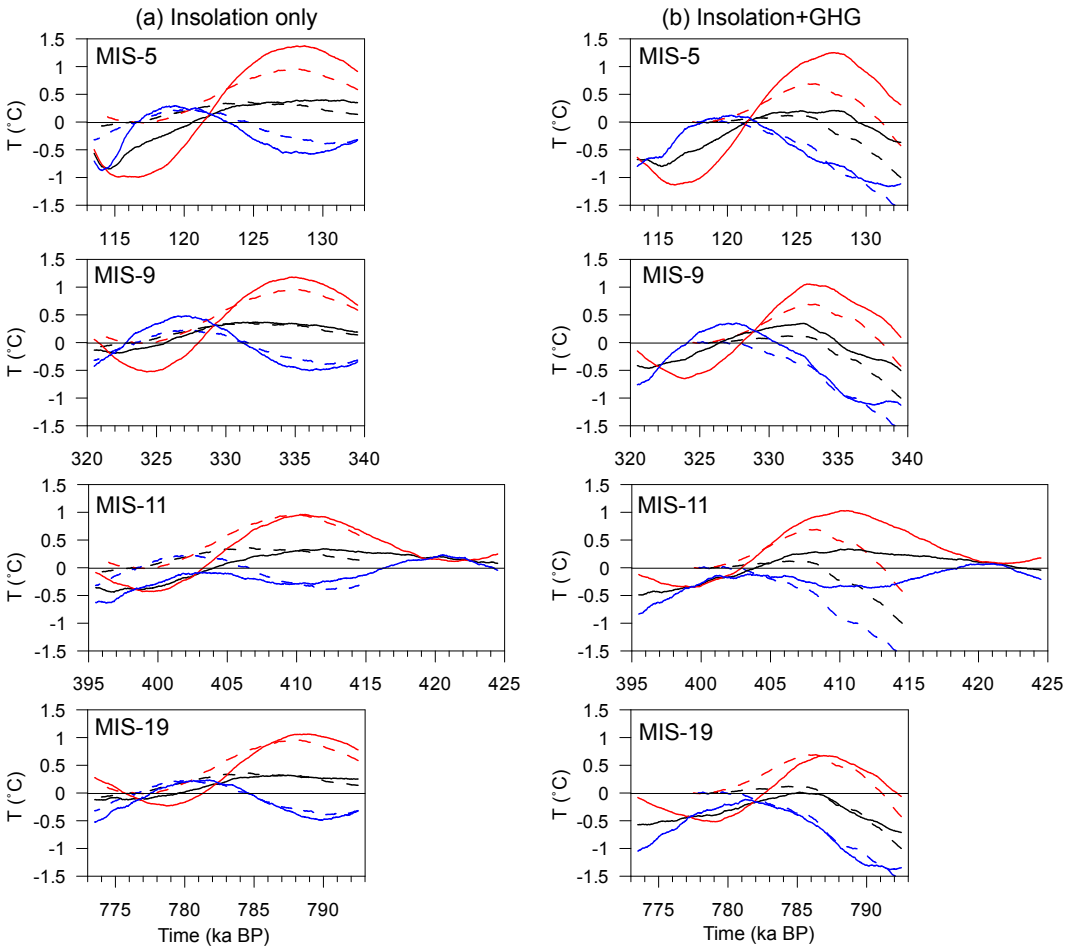

Fig. 12. Global mean surface air temperature (°C) relative to PI for annual mean (black), JJA (red) and DJF (blue). (a) Results of the transient simulations where time-varying insolation is used and CO_2 is fixed to 280 ppmv; and (b) results of the transient simulations where both insolation and CO_2 vary with time. MIS-1 is in dashed line, and its time interval is from 17 ka BP to 3 ka AP in (a) and from 17 ka BP to present in (b). The other four interglacials are in solid line. The five interglacials are aligned according to precession. The 1000-year running mean of temperature is plotted.

high CO_2 concentration, the transient simulation shows that MIS-11 is warmer than MIS-1 for both the annual and seasonal temperatures.

8. Conclusions

The search for Late Pleistocene analogues of the future climate, natural and hopefully under human activities, led us to analyse the warm interglacials of the last 800 ka. Given the projected exceptional warmth over the next centuries, a particular attention was paid to the warmest interglacials, i.e. MIS-1, MIS-5, MIS-9, MIS-11 and MIS-19, although it must be stressed that their astronomical configurations are not the same as for the present-day and the near future and their CO_2 concentration is much lower.

Two sets of snapshot simulations with the insolation taken when NH summer occurs at perihelion (NHSP) and at the interglacial $\delta^{18}O$ peaks respectively allowed looking first for analogues of the Holocene Optimum. In the NHSP experiments, MIS-19 appears to be the best analogue of MIS-1, in terms of the CO_2 concentration, the latitudinal and seasonal distribution of insolation and the climate response to these forcings. The combined effect of insolation and CO_2 on the climate of MIS-11 is also similar to MIS-1 but its origin is different: MIS-11 is cooler than MIS-1 for its insolation but warmer for its CO_2 concentration. Although MIS-1, MIS-11 and MIS-19 all have a low eccentricity related to the 400-ka cycle of eccentricity, MIS-11 departs from MIS-1 and MIS-19 mainly because of its lower obliquity at the time of NHSP. MIS-5 and MIS-9 are much warmer than MIS-1 during boreal summer and much cooler during boreal winter, leading to a very strong seasonal contrast. At the annual scale, they are warmer than MIS-1 over most of the Globe, particularly over the high latitudes. The interglacial $\delta^{18}O$ peaks are characterized by NH fall occurring at perihelion and obliquity smaller than at NHSP. This explains that their simulated climate is obviously cooler in the mid-high latitudes of both hemispheres and warmer in the tropics than the climate of NHSP. Using the interglacial $\delta^{18}O$ peaks, no analogue of MIS-1 can be found. Comparison between model results and proxy data shows that the insolation of NHSP is a better choice for simulating the interglacial climate “Optimum” when snapshot simulations are made.

To overcome the weakness of using one single date for representing one interglacial and to avoid the equilibrium climate hypothesis, transient simulations were made. Such transient simulations, which cover a full spectrum of astronomical configurations during the entire period of each interglacial, allow comparing the interglacials between them together and looking for the analogues of the whole Holocene and its natural future. Based on these simulations, an OPE (obliquity-precession-eccentricity) index has been developed to estimate the climate sensitivity to astronomical forcing. They also show that obliquity and precession

have different weight on the annual mean temperature and precipitation of different latitudinal zones, therefore the climates of different latitudes are not necessarily in phase. The response of the climate system is shown to depend strongly upon the phase between obliquity and precession. When obliquity maximum occurs with the NH summer being at perihelion (i.e. precession minimum), as it is for MIS-9, MIS-19 and almost for MIS-1, the maximum temperature of the NH mid-high latitudes occurs about 5 ka earlier than in the SH because of the higher sensitivity of the vast continental areas of the NH. When the obliquity maximum happens only a few thousands of years before precession minimum, like for MIS-5, the responses of the mid-high latitudes of the two hemispheres are more or less in phase, the huge capacity of the Southern Ocean delaying the expected early response of the SH to obliquity. When obliquity maximum and precession minimum are almost in anti-phase, like for MIS-11, the maximum in the annual mean temperature of the SH mid and high latitudes occurs a few thousands of years earlier than in the NH, expressing the larger sensitivity of the SH to obliquity.

The phase difference of the temperature and precipitation between different latitudinal zones and between them and precession/obliquity means that one must be very cautious when astronomically tuning the chronology of a proxy record or tuning it to a proxy from other regions. However, our transient simulations show that the JJA temperature of different latitudinal zones (except the Southern Oceans) are all in phase and dominated by precession, their maxima occurring when NH summer insolation reaches its maximum. This suggests that the JJA temperature could be used easily and confidently in the intercomparison between different regions and between different interglacials and therefore between the related proxies.

Compared to the natural climate of the present-day and its near future, the past interglacials are warmer during boreal summer and cooler during boreal winter leading to a stronger seasonal contrast and a warmer annual mean. The warm interval of MIS-11 is the longest, confirming the long duration of this interglacial as found in proxy studies. It is related to the long-lasting low eccentricity and high CO_2 concentration and to the anti-phase relationship between obliquity maximum and precession minimum during MIS-11. This exceptional phase relationship between obliquity and precession might also explain the simulated simultaneous occurrence of warm winters and warm summers in the Arctic. Such occurrence, with at the same time, the appearance of a warm winter and a moderately cool summer over Antarctica and its surrounding oceans might be at the origin of a particularly large sea-level rise during MIS-11, which remains to be confirmed by ice sheet modelling.

When considering the variations in both annual and seasonal temperatures over the whole interval of each interglacial, our simulations show that MIS-19 is the best analogue of the Holocene and its natural near future. MIS-11 is close to the Holocene when the impact of insolation alone is considered, but its long lasting high CO_2 concentration makes it warmer. Due to the large amplitude of variations in insolation and also to their higher CO_2 concentration, MIS-5 and MIS-9 can hardly be considered as analogue of the Holocene. However, their warm climates as well as the climate of MIS-11 make them the closest to the future human-induced warm climate. Indeed, although their astronomical forcing is different from the future and their CO_2 concentration is much lower than the anthropogenic CO_2 concentration, there are similarities between the past warm interglacials and the anthropogenic warming in terms of climate feedbacks at the regional scale. In both cases, the largest climate change happens at high latitudes of both hemispheres related to the positive snow-ice-albedo-temperature feecbacks, and the seasonal response over the polar oceans is asymmetric. For the past interglacials, the local winter over the polar oceans is indeed directly influenced by the local summer through the summer remnant effect of insolation as explained in Yin and Berger (2012). Similar mechanisms related to the atmosphere-ocean-sea ice interactions are also found in the present global warming resulting from the anthropogenic CO_2 increase (Manabe and Stouffer, 1980).

The differences between the seasonal behaviours of the past interglacials and of the present-day and its near future leads to stress the importance of reconstructing the seasonal climate from proxy records and therefore the need to find proxies sensitive to the seasonal cycle. Regarding the analogue of the natural climate of the present-day and of the next centuries, the climate simulated at the $\delta^{18}O$ peak of MIS-19 is found to be the best choice. The natural future climate provides the background over which the impacts of human activities can be assessed.

Acknowledgements

This paper is dedicated to Dr George Kukla who passed away on 31 May 2014 and devoted all his life to paleoclimate research and in particular to the interglacials. This work was supported by the European Research Council Advanced Grant EMIS (No. 227348 of the Programme 'Ideas') and partly and more recently by the Natural Science Foundation of China (NSFC, No. 41430103). Q.Z.Yin is supported by the Belgian National Fund for Scientific Research (F.R.S.-FNRS). Access to computer facilities was made easier through sponsorship from S. A. Electrabel, Belgium. The authors thank CISM staff and Pierre-Yves Barriat at Université catholique de Louvain for technical support and two reviewers for their constructive comments.

References

Bauch, H.A., Erlenkeuser, H., Helmke, J.P., Struck, U., 2000. A paleoclimatic evaluation of marine oxygen isotope stage 11 in the high-northern Atlantic (Nordic seas). Glob. Planet. Chang. 24, 27–39.

Berger, A., 1978. Long-term variations of daily insolation and Quaternary climatic changes. J. Atmos. Sci. 35 (12), 2362–2367.

Berger, A., 1989. Response of the climate system to CO_2 and astronomical forcings. In: Paleo-analogs, IPCC Working Group I, Bath, 20–21 November 1989.

Berger, A., Loutre, M.F., 1994. Long-term variations of the astronomical seasons. In: Boutron, Cl (Ed.), Topics in Atmospheric and Interstellar Physics and Chemistry. Les Editions de Physique, Les Ulis, France, pp. 33–61.

Berger, A., Loutre, M.F., 1996. Modelling the climate response to astronomical and CO_2 forcings. C. R. Acad. Sci. Paris 323, 1–16.

Berger, A., Loutre, M.F., 2002. An exceptionally long interglacial ahead? Science 297, 1287–1288.

Berger, A., Loutre, M.F., 2003. Climate 400,000 years ago, a key to the future? In: Droxler, A., Burckle, L., Poore, A. (Eds.), Earth Climate and Orbital Eccentricity: the Marine Isotope Stage 11 Question, Geophysical Monograph, vol. 137. American Geophysical Union, pp. 17–26.

Berger, A., Loutre, M.F., Melice, J.L., 2006. Equatorial insolation: from precession harmonics to eccentricity frequencies. Clim. Past. 2, 131–136.

Berger, A., Loutre, M.F., Yin, Q.Z., 2010. Total irradiation during any time interval of the year using elliptic integrals. Quat. Sci. Rev. 29, 1968–1982.

Berger, A., 2012. A brief history of the astronomical theories of paleoclimates. In: Berger, A., Mesinger, F., Sijacki, D. (Eds.), Climate Change at the Eve of the Second Decade of the Century. Inferences from Paleoclimates and Regional Aspects, Proceedings of Milankovitch 130th Anniversary Symposium. Springer-Verlag/Wien, pp. 107–129. http://dx.doi.org/10.1007/978-3-7091-0973-1.

Braconnot, P., Otto-Bliesner, B., Harrison, S., et al., 2007. Results of PMIP2 coupled simulations of the Mid-Holocene and Last Glacial Maximum. Part 1: experiments and large-scale features. Clim. Past. 3, 261–277.

CAPE-Last Interglacial Project Members, 2006. Last Interglacial Arctic warmth confirms polar amplification of climate change. Quat. Sci. Rev. 25, 1383–1400.

Chen, G.S., Kutzbach, J.E., Gallimore, R., Liu, Z., 2011. Calendar effect on phase study in paleoclimate transient simulation with orbital forcing. Clim. Dyn. 37 (9–10), 1949–1960.

De Vernal, A., Hillaire-Marcel, C., 2008. Natural variability of Greenland climate, vegetation, and ice volume during the past million years. Science 320, 1622–1625.

Droxler, A., Poore, R.Z., Burckle, L.H., 2003. Earth's Climate and Orbital Eccentricity. In: Geophysical Monograph, vol. 137. American Geophysical Union, Washington D.C, ISBN 0-87590-996-5, p. 240.

Ganopolski, A., Calov, R., 2011. The role of orbital forcing, carbon dioxide and regolith in 100 kyr glacial cycles. Clim. Past. 7, 1415–1425.
Ganopolski, A., Robinson, A., 2011. The past is not the future. Nat. Geosci. 4, 661–663. http://dx.doi.org/10.1038/ngeo1268.
Goelzer, H., Huybrechts, P., Loutre, M.F., Goosse, H., Fichefet, T., Mouchet, A., 2010. Impact of Greenland and Antarctic ice sheet interactions on climate sensitivity. Clim. Dyn. http://dx.doi.org/10.1007/s00382-010-0885-0.
Goosse, H., Brovkin, V., Fichefet, T., Haarsma, R., Huybrechts, P., Jongma, J., Mouchet, A., Selten, F., Barriat, P.Y., Campin, J.M., Deleersnijder, E., Driesschaert, E., Goelzer, H., Janssens, I., Loutre, M.F., Morales, Maqueda, M.A., Opsteegh, T., Mathieu, P.P., Munhoven, G., Petterson, J.E., Renssen, H., Roche, D., Schaeffer, M., Tartinville, B., Timmermann, A., Weber, S.L., 2010. Description of the earth system model of intermediate complexity LOVECLIM version 1.2. Geosci. Model Dev. 3, 603–633.
Herold, N., Yin, Q.Z., Karami, P., Berger, A., 2012. Modeling the climatic diversity of the warm interglacials. Quat. Sci. Rev. 56, 126–141.
Hodell, D.A., Charles, C.D., Ninnemann, U.S., 2000. Comparison of interglacial stages in the South Atlantic sector of the southern ocean for the past 450 kyr: implications for marine isotope stage_MIS/11. Glob. Planet. Chang. 24, 27–26.
Hewitt, C.D., Mitchell, J.F.B., 1998. A fully coupled GCM simulation of the climate of the mid-Holocene. Geophys. Res. Lett. 25 (3), 361–364.
Imbrie, J., Imbrie, K.P., 1979. Ice Ages: Solving the Mystery. Enslow, Springfield, N. J, p. 224.
IPCC, 2013. Climate change 2013: the physical science basis. Contribution of working group I to the fifth assessment report of the intergovernmental panel on climate change. In: Stocker, T.F., Qin, D., Plattner, G.K., Tignor, M., Allen, S.K., Boschung, J., Nauels, A., Xia, Y., Bex, V., Midgley, P.M. (Eds.). Cambridge University Press, Cambridge, United Kingdom and New York, NY, USA, p. 1535.
Joussaume, S., Taylor, K.E., 1995. Status of the paleoclimate modeling intercomparison project (PMIP). In: Proceedings of the First International AMIP Scientific Conference, pp. 425–430. WCRP Report.
Joussaume, S., Braconnot, P., 1997. Sensitivity of paleoclimate simulation results to season definitions. J. Geophys. Res. Atmos. 102 (D2), 1943–1956.
Jouzel, J., Masson-Delmotte, V., Cattani, O., Dreyfus, G., Falourd, S., Hoffmann, G., Minster, B., Nouet, J., Barnola, J.M., Chappellaz, J., Fischer, H., Gallet, J.C., Johnsen, S., Leuenberger, M., Loulergue, L., Luethi, D., Oerter, H., Parrenin, F., Raisbeck, G., Raynaud, D., Schilt, A., Schwander, J., Selmo, E., Souchez, R., Spahni, R., Stauffer, B., Steffensen, J.P., Stenni, B., Stocker, T.F., Tison, J.L., Werner, M., Wolff, E.W., 2007. Orbital and millennial Antarctic climate variability over the past 800,000 years. Science 317, 793–796.
Kleinen, T., Brovkin, V., von Bloh, W., Archer, D., Munhoven, G., 2010. Holocene carbon cycle dynamics. Geophys. Res. Lett. 37 (2) http://dx.doi.org/10.1029/2009GL041391.
Kopp, R.E., Simons, F.J., Mitrovica, J.X., Maloof, A.C., Oppenheimer, M., 2009. Probabilistic assessment of sea level during the Last Interglacial stage. Nature 462, 863–867.
Kukla, G., 2003. Continental records of MIS 11. In: Droxler, A., Burckle, L., Poore, A. (Eds.), Earth Climate and Orbital Eccentricity: the Marine Isotope Stage 11 Question, Geophysical Monograph, vol. 137. American Geophysical Union, pp. 207–212.
Kukla, G., Berger, A., Lotti, R., Brown, J., 1981. Orbital signature of interglacials. Nature 290, 295–300.
Kukla, G., McManus, J.F., Rousseau, D.D., Chuine, I., 1997. How long and how stable was the Last Interglacial? Quat. Sci. Rev. 16 (6), 605–612.
Kutzbach, J., 1981. Monsoon climate of the Early Holocene: climate experiment with the earth's orbital parameters for 9000 years ago. Science 214, 59–61.
Lang, N., Wolff, E.W., 2011. Interglacial and glacial variability. Clim. Past. 7, 361–380.
Lea, D.W., Pak, D.K., Spero, H.J., 2003. Sea surface temperatures in the western Equatorial Pacific during marine isotope stage 11. In: Droxler, A., Burckle, L., Poore, A. (Eds.), Earth Climate and Orbital Eccentricity: the Marine Isotope Stage 11 Question, Geophysical Monograph, vol. 137. American Geophysical Union, pp. 147–156.
Lisiecki, L.E., Raymo, M.E., 2005. A Pliocene-Pleistocene stack of 57 globally distributed benthic delta δ18O records. Paleoceanography 20 (1), PA1003. http://dx.doi.org/10.1029/2004PA001071.
Lorenz, S., Lohmann, G., 2004. Acceleration technique for Milankovitch type forcing in a coupled atmosphere-ocean circulation model: method and application for the Holocene. Clim. Dyn. 23 (7–8), 727–743.
Loutre, M.F., Fichefet, T., Goosse, H., Huybrechts, P., Goelzer, H., Capron, E., 2014. Factors controlling the last interglacial climate as simulated by LOVECLIM1.3. Clim. Past. Discuss. 10, 235–290.
Loutre, M.F., Berger, A., 2003. Marine Isotope Stage 11 as an analogue for the present interglacial. Glob. Planet. Change 36, 209–217.
Lunt, D.J., Abe-Ouchi, A., Bakker, P., Berger, A., Braconnot, P., Charbit, S., Fischer, N., Herold, N., Jungclaus, J.H., Khon, V.C., Krebs-Kanzow, U., Langebroeck, P.M., Lohmann, G., Nisancioglu, K.H., Otto-Bliesner, B.L., Park, W., Pfeiffer, M., Phipps, S.J., Prange, M., Rachmayani, R., Renssen, H., Rosenbloom, N., Schneider, B., Stone, E.J., Takahashi, K., Wei, W., Yin, Q., Zhang, Z.S., 2013. A multi-model assessment of last interglacial temperatures. Clim. Past. 9, 699–717.
Luthi, D., Le Floch, M., Bereiter, T., Barnola, J.-M., Siegenthaler, U., Raynaud, D., Jouzel, J., Fisher, H., Kawamura, K., Stocker, T.F., 2008. High-resolution carbon dioxide concentration record 650,000-800,000 years before present. Nature 453, 379–382.
Manabe, S., Stouffer, R.J., 1980. Sensitivity of a global climate model to an increase of CO_2 concentration in the atmosphere. J. Geophys Res. 85, 5529–5554.
Masson-Delmotte, V., Stenni, B., Pol, K., Braconnot, P., Cattani, O., Falourd, S., Kageyama, M., Jouzel, J., Landais, A., Mi nster, B., Krinner, G., Johnsen, S., Röthlisberger, R., Chappellaz, J., Hansen, J., Mikolajewicz, U., Otto-Bliesner, B., 2010. EPICA Dome C record of glacial and interglacial intensities. Quat. Sci. Rev. 29, 113–128.
McManus, J., Oppo, D., Cullen, J., Healey, S., 2003. Marine isotope stage 11 (MIS 11): analog for holocene and future climate? In: Droxler, A., Burckle, L., Poore, A. (Eds.), Earth Climate and Orbital Eccentricity: the Marine Isotope Stage 11 Question, Geophysical Monograph, vol. 137. American Geophysical Union, pp. 69–85.
McManus, J.F., Oppo, D.W., Cullen, J.L., 1999. A 0.5-Million-Year record of millennial-scale climate variability in the North Atlantic. Science 283, 971–975.
NEEM community members, 2013. Eemian interglacial reconstructed from a Greenland folded ice core. Nature 493, 489–494.
Olson, S.L., Hearty, P.J., 2009. A sustained t21 m sea-level highstand during MIS 11 (400ka): direct fossil and sedimentary evidence from Bermuda. Quat. Sci. Rev. 28, 271–285.
Otto-Bliesner, B.L., Marshall, S.J., Overpeck, J.T., Miller, G.H., Hu, A., CAPE Last Interglacial Project members, 2006. Arctic warmth and the Greenland ice sheet during the Last Interglaciation. Science 311, 1751–1753.
Pol, K., Masson-Delmotte, V., Johnsen, S., Bigler, M., Cattani, O., Durand, G., Falourd, S., Jouzel, J., Minster, B., Parrenin, F., Ritz, C., Steen-Larsen, H.C., Stenni, B., 2010. New MIS 19 EPICA Dome C high resolution deuterium data: hints for a problematic preservation of climate variability at sub-millennial scale in the "oldest ice". Earth Planet. Sci. Lett. 298, 95–103.
Raymo, M., Mitrovica, X., 2012. Collapse of polar ice sheets during the stage 11 interglacial. Nature 483, 453–456.
Renssen, H., Seppa, H., Heiri, O., Roche, D.M., Goosse, H., Fichefet, T., 2009. The spatial and temporal complexity of the Holocene thermal maximum. Nat. Geosci. 2, 411–414.
Rousseau, D.D., 2003. The continental record of stage 11: a review. In: Droxler, A., Burckle, L., Poore, A. (Eds.), Earth Climate and Orbital Eccentricity: the Marine Isotope Stage 11 Question, Geophysical Monograph, vol. 137. American Geophysical Union, pp. 213–222.
Ruddiman, W.F., 2007. The early anthropogenic hypothesis: challenges and responses. Rev. Geophys. 45, RG4001.
Timm, O., Timmermann, A., 2007. Simulation of the last 21 000 years using accelerated transient boundary conditions. J. Clim. 20, 4377–4401.
Timm, O., Timmermann, A., Abe-Ouchi, A., Saito, F., Segawa, T., 2008. On the definition of seasons in paleoclimate simulations with orbital forcing. Paleoceanography 23, PA2221. http://dx.doi.org/10.1029/2007PA001461.
Turney, C.S.M., Jones, R.T., 2010. Does the Agulhas current amplify global temperatures during super-interglacials? J. Quat. Sci. 25, 839–843.
Tzedakis, P.C., Raynaud, D., McManus, J.F., Berger, A., Brovkin, V., Kiefer, T., 2009. Interglacial diversity. Nat. Geosci. 2 (11), 751–755.
Tzedakis, P.C., 2010. The MIS 11-MIS 1 analogy, southern European vegetation, atmospheric methane and the "early anthropogenic hypothesis". Clim. Past. 6, 131–144.
Tzedakis, P.C., Channell, J.E.T., Hodell, D.A., Kleiven, H.F., Skinner, L.C., 2012. Determining the natural length of the current interglacial. Nat. Geosc 5 (2), 138–142.
Van de Berg, W.J., van den Broeke, M., Ettema, J., van Meijgaard, E., Kaspar, F., 2011. Significant contribution of insolation to Eemian melting of the Greenland ice sheet. Nat. Geosci. 4, 679–683. http://dx.doi.org/10.1038/ngeo1245.
Wang, X., Auler, A.S., Edwards, R.L., Cheng, H., Cristalli, P.S., Smart, P.L., Richards, D.A., Shen, C.-C., 2004. Wet periods in northeastern Brazil over the past 210 kyr linked to distant climate anomalies. Nature 432, 740–743.
Yin, Q.Z., Berger, A., 2010. Insolation and CO_2 contribution to the Interglacial climate before and after the Mid-Brunhes event. Nat. Geosci. 3 (4), 243–246.
Yin, Q.Z., 2013. Insolation-induced mid-Brunhes transition in Southern Ocean ventilation and deep-ocean temperature. Nature 494, 222–225. http://dx.doi.org/10.1038/nature11790.
Yin, Q.Z., Berger, A., 2012. Individual contribution of insolation and CO_2 to the interglacial climates of the past 800,000 years. Clim. Dyn. 38, 709–724.